

EFFECT OF RIGID ROD MOLECULAR STRUCTURES ON THE  
PROPERTIES OF REGENERATED AND VIRGIN  
POLY(ETHYLENE TEREPHTALATE)

A THESIS SUBMITTED TO  
THE GRADUATE SCHOOL OF NATURAL AND APPLIED SCIENCES  
OF  
MIDDLE EAST TECHNICAL UNIVERSITY

BY

C. ZEYNEP DURU

IN PARTIAL FULFILLMENT OF THE REQUIREMENTS FOR THE  
DEGREE OF MASTER OF SCIENCE  
IN  
POLYMER SCIENCE AND TECHNOLOGY

SEPTEMBER,2004

Approval of the Graduate School of Natural and Applied Sciences

---

Prof. Dr. Canan ÖZGEN  
Director

I certify that this thesis satisfies all the requirements as a thesis for the degree of Master of Sciences.

---

Prof. Dr. Ali USANMAZ  
Head of Department

This is to certify that we have read this thesis and that in our opinion it's fully adequate, in scope and quality, as a thesis for the degree of Master of Science.

---

Prof. Dr. Erdal BAYRAMLI  
(Supervisor)

Examining Committee in Charge

Prof. Dr. Ülkü Yılmaz (METU,CHEM.ENG.)

---

Prof. Dr. Erdal Bayramlı (METU,CHEM)

---

Prof. Dr. Serpil Aksoy (GAZİ UNI.,CHEM)

---

Prof. Dr. Ahmet Önal (METU,CHEM)

---

Assoc.Prof.Dr. Zeki Öktem (KRK.UN.,CHEM)

---

**I hereby declare that all information in this document has been obtained and presented in accordance with academic rules and ethical conduct. I also declare that, as required by these rules and conduct, I have fully cited and referenced all material and results that are not original to this work.**

Name, Last name : C.Zeynep Duru

Signature :

## ABSTRACT

### EFFECT OF RIGID ROD MOLECULAR STRUCTURES ON THE PROPERTIES OF REGENERATED AND VIRGIN POLY(ETHYLENE TEREPHTHALATE)

DURU, Zeynep

M.S., Department of Polymer Science and Technology

Supervisor Prof.Dr.Erdal Bayramlı

September 2004, 73 pages

In recent years, the recycling of plastic waste increased worldwide. The basic impetus for this increase is the public awareness regarding pollution of the environment. Many different types of recycling processes are being used to reduce the use of raw materials and to reduce energy consumption. PET recycling is one of the most important recycling processes.

Addition of thermotropic liquid crystalline polymers to common commodity polymers has also become wide-spread in recent years to increase their mechanical properties and other selected properties. In this study, it is aimed to obtain a continuous or discontinuous fiber from the thermotropic liquid crystalline copolyester and recycled PET blend. In this study X7G (60%PABA/40%PET) was used as a copolyester. In the polymer mixtures

small amounts of liquid crystalline polymer phase resulted in significant improvements in the mechanical properties of the fibers produced in the study. The blending method used gave an almost homogeneous polymer mixture which was unexpected that needs further study to elaborate. The preliminary DSC, SEM, tensile testing and intrinsic viscosity measurements support this conclusion. The material obtained approached to fiber grade PET in terms of fiber forming properties which therefore can be used as a second grade fiber material.

Keywords: Recycling, liquid crystalline copolyesters, fibers, blends

## ÖZ

### BÜKÜLMEZ ÇUBUK ŞEKLİNDEKİ MOLEKÜLLERİN REJENERE VE İŞLENMEMİŞ POLY(ETİLEN TERAFİTALAT) ÖZELLİKLERİNE ETKİSİ

DURU, Zeynep

Yüksek Lisans, Polimer Bilim ve Teknolojisi Bölümü

Tez Yöneticisi Prof.Dr. Erdal Bayramlı

Eylül 2004, 73 sayfa

Son yıllarda tüm dünyada plastiklerin geri dönüşüm işlemi artmıştır. Bu artıştaki en büyük neden toplumda çevre duyarlılığının artmış olmasıdır. Hammadde ve enerji tüketimini azaltmak amacıyla çok çeşitli geri dönüşüm işlemleri uygulanmaktadır. PET geri dönüşümü ise geri dönüşüm işleminin en önemlilerinden biridir.

Son yıllarda termotropik sıvı kristal polimerlerin genel amaçlı yaygın kullanılan polimerlere katılması yoluyla istenen mekanik ve diğer özelliklerin kazanılması yoluna gidilmesi oldukça yaygınlaşmıştır. Bu çalışmada, termotropik sıvı kristal kopoliester ve rejenere PET karışımından kesikli ya da devamlı elyaf üretimi amaçlanmıştır. Çalışmada sıvı kristal kopoliester olarak X7G (60%PABA/40%PET) kullanılmıştır. Polimer karışımlarına az miktarda sıvı kristal kopoliesterin eklenmesi ile üretilen elyafların mekanik özelliklerinde önemli gelişme sağlanmıştır. Kullanılan karıştırma metodu, beklenmeyen bir şekilde homojen görünen bir karışım vermiştir. Bu bulgunun

daha detaylı çalıřmalarla desteklenmesi gerekmektedir. Bu arařtırmada yapılan DSC, SEM, mekanik testleri ve viskosite ölçümleri de bu sonucu desteklemektedir.Elyaf oluřturma özelliđi aısından elde edilen materyal ikinci sınıf bir elyaf oluřturmak üzere kullanılabilir.

Anahtar Kelimeler: Geri dönüşüm, PET, Sıvı kristal kopoliesterler, Elyaf, Karıřım.

## ACKNOWLEDGEMENTS

First of all, I would like to express my great gratitude to Prof.Dr. Erdal Bayramlı who has given me a chance of being his student and during my study he enlightened me with his deep knowledge besides this he also encourage me in all other skills,

Special thanks for Assoc.Prof.Dr.ZekeriyaYerlikaya for his valuable support,especially when composing my fibers and making their characterization analysis,

And I would to thank to Asst. Güralp Özkoç who guided tensile tests with a wonderful motivation in the Experimental Mechanical Laboratory of the department of Engineering Science,

And Asst. Prof. Dr. Ayşen Yılmaz who gave me support during my X-ray analysis,

And to all Polymer Science and Technology Department, especially the technicians who solved the mechanical problems of the instruments,

And to my room-mates also my friends Tuncay Baydemir, Yasin Ağırtopçu, Selahattin Erdoğan, Mustafa Balgat for their support and help during this program,

Finally, I want to thank my family for their support during my whole education.

## TABLE OF CONTENTS

PLAGIARISM.....	iii
ABSTRACT.....	iv
ÖZ .....	vi
ACKNOWLEDGEMENTS.....	viii
TABLE OF CONTENTS .....	ix
LIST OF TABLES .....	xv
ABBREVIATIONS.....	xvi
CHAPTER 1 .....	1
INTRODUCTION.....	1
1.1 LIQUID CRYSTALLINE POLYMERS.....	1
1.1.1 Thermotropic Liquid Crystalline Polymers .....	2
1.1.1.1 Properties of Thermotropic LCPs .....	3
1.1.2 LCP Blends and Effect of LCPs on Morphological Behavior of PET.....	4
1.2 RECYCLING AND RECYCLED PET .....	6
1.2.1 Recycling and Importance of Recycling .....	6
1.2.2 Methods And Uses For Recycling PET .....	10
1.3 PET and LCP BLENDS.....	11
1.3.1 Fibrillation .....	11

1.3.2	Fibers from Liquid Crystalline Polymers .....	11
1.3.3	HBA / PET Copolyester Fiber Structure, Morphology and Properties .....	15
1.3.4	Wind Up Speed Suppression (WUSS) Effect.....	17
1.4	Scope of Work .....	18
CHAPTER 2	.....	19
EXPERIMENTAL	.....	19
2.1	MATERIALS.....	19
2.2	Synthesis of X7G .....	19
2.3	Preparation of PET and LCP (X7G) Blends.....	21
2.4	FIBER FORMATION PROCESS .....	23
2.4.1	Fiber Spinning.....	23
2.5	DRAWING PROCESS .....	27
2.6	CHARACTERIZATION METHODS .....	28
2.6.1	Melt Flow Index Measurements .....	28
2.6.2	Solution Viscosity Measurements.....	30
2.6.3	Differential Scanning Calorimetry .....	32
2.6.4	Scanning Electron Microscopy .....	33
2.6.5	Fiber Tensile Test.....	33
2.6.6	Wide Angle X- Ray Diffraction (WAXD) Analysis.....	35
CHAPTER 3	.....	37
RESULTS AND DISCUSSION	.....	37
3.1	Melt Flow Index Results.....	37
3.2	Solution Viscosity Results.....	39

3.3	DSC Results.....	40
3.4	SEM Results.....	54
3.5	Tensile Properties of the Fibers .....	60
3.6	Wide Angle X- Ray Test Results.....	64
	CONCLUSIONS.....	66
	REFERENCES .....	68
	APPENDIX.....	72
	Tensile Strength Values.....	72

## LIST OF FIGURES

Figure 1.1 Structure of X7G copolyester .....	17
Figure 2.1 Polymerization and Blending System .....	22
Figure 2.2 Spiral mixing head of the Reactor.....	23
Figure 2.3 Engineering Drawing of Midi - Melt Extruder.....	26
Figure 2.4 Drawing System .....	27
Figure 2.5 Fiber Holder .....	28
Figure 2.6 Melt Flow Index Instrument .....	29
Figure 2.7 Single Fiber Specimen Mounting Set-up .....	35
Figure 3.1 DSC Thermogram of Fiber Grade PET (FGPET) .....	42
Figure 3.2a DSC Thermogram of Spun Fiber from FGPET .....	43
Figure 3.2b DSC Thermogram of Drawn Fiber from FGPET .....	44
Figure 3.3 DSC Thermogram of Bottle Grade PET (BGPET).....	45
Figure 3.4 DSC Thermogram of Spun Fiber from BGPET .....	46
Figure 3.5 DSC Thermogram of BGPET +1% LCP Blend Fiber .....	49
Figure 3.6 DSC Thermogram of BGPET + 2% LCP Blend Fiber .....	50
Figure 3.7 DSC Thermogram of Recycled PET (R-PET).....	51
Figure 3.8 DSC Thermogram of R- PET + 1% LCP Blend Fiber.....	52
Figure 3.9 DSC Thermogram of R-PET + 2% LCP Blend Fiber.....	53

Figure 3.10 SEM Microphotograph of the fiber from FGPET.....	54
Figure 3.11 SEM Microphotograph of FGPET fiber with lamellar structure..	55
Figure 3.12 SEM Microphotograph of the fiber from BGPET .....	55
Figure 3.13 SEM Microphotograph of the fiber from BGPET with smooth skin .....	56
Figure 3.14 SEM Microphotograph of the fiber from BGPET with ductile rupture.....	56
Figure 3.15 SEM Microphotograph of the fiber from BGPET+ 1%LCP with lamellar structure.....	57
Figure 3.16 SEM Microphotograph of the fiber from BGPET+1%LCP blend fiber that shows fibrillation.....	58
Figure 3.17 SEM Microphotograph of a thin R-PET fiber. ....	58
Figure 3.18 SEM Microphotograph of R-PET fiber with no lamellar structure. .....	59
Figure 3.19 SEM Microphotograph of a collection of R-PET fibers. ....	59
Figure 3.20 Stress-strain curves for R-PET, FGPET and R-PET+1%LCP blend fibers.....	61
Figure 3.21 Variation of tensile strengths for R-PET, FGPET and R-PET +1%LCP blend fibers .....	62

Figure 3.22 Variations of strain at break values for R-PET,FGPET and R- PET+1%LCP blend fibers .....	63
Figure 3.23 Variation of tensile modulus for R-PET, FGPET and R-PET +1%LCP blend fibers .....	64
Figure 3.24 WAXD spectrum of R-PET +1% LCP; intensity vs. $2\theta$ .....	65

## LIST OF TABLES

Table 1.1 Growth of plastics in MSW in USA.....	7
Table 1.2 Most Popular PET Waste Treatment Methods .....	10
Table 3.1 Melt Flow Index Values of PET and PET-LCP Blends .....	38
Table 3.2 Intrinsic Viscosity Results of the Bottle Grade PET, Recycled PET and their Blends with LCP.....	39
Table 3.3 $T_{cry}$ and $T_m$ values of the Samples .....	41
Table 3.4 Maximum Tensile Strength and % Strain at Break Values of the Fibers .....	60

## ABBREVIATIONS

PET	Poly(ethyleneterephthalate)
LCP	Liquid crystalline polymer
TLCP	Thermotropic liquid crystalline polymer
PP	Polypropylene
PVC	Polyvinylchloride
EG	Ethylene glycol
HBA	Hydroxybenzoicacid
BHET	Bishydroxyethylterephthalate
WUSS	Wind-up speed suppression
PABA	paraacetoxybenzoicacid
MFI	Melt flow index
BGPET	Bottle grade PET
FGPET	Fiber grade PET
R-PET	Recycled PET
DSC	Differential Scanning Calorimetry
SEM	Scanning Electron Microscopy
MFI	Melt Flow Index
WAXD	Wide Angle X-Ray Diffraction
X7G	60%PABA/40%PET copolyester
T <sub>cry</sub>	Crystallization temperature
T <sub>m</sub>	Melting temperature

## **CHAPTER 1**

### **INTRODUCTION**

#### **1.1 LIQUID CRYSTALLINE POLYMERS**

A liquid crystal is a state of matter between the liquid and crystal states. Liquid crystals are ordered like crystals but flow like liquids. Liquid crystals are either thermotropic, which means that they are liquid crystalline in the temperature range between melt and solid states, or lyotropic, which means that they form liquid crystals in the concentrated solutions.

In last two decades, a new class of thermotropic polymeric materials known as liquid crystalline polymers (LCPs) has been developed as a new type material. LCPs are an important extension to science and technology. These polymers usually consist of rigid rodlike molecular chains and they are capable of forming highly oriented structures with strength and moduli significantly higher than those of the conventional polymers within standard polymer matrices, such as PET, LCP's form composite-like structures where LCPs serve as the reinforcing component [1].

Conventional amorphous, crystalline and partially crystalline synthetic polymers have become highly important materials. Liquid crystalline polymers, offer many potential applications and their applications arise from a

number of interesting properties they exhibit including; low melt viscosity, very low mold shrinkage, excellent mechanical properties and good solvent resistance [2].

### **1.1.1 Thermotropic Liquid Crystalline Polymers**

Thermotropic liquid phases occurs in both pure compounds and mixtures. The unusual rheological and mechanical properties of thermotropic liquid crystalline polymers are well known. The nematic ordered structure is responsible for the low melt viscosity and the high degree of orientation that can be achieved under elongational flow [3].

Thermotropic liquid crystalline copolymers exhibit a high degree of molecular orientation during processing in the melt state and are able to maintain this orientation during solidification. Relatively rigid backbone molecules produce anisotropic or orthotropic structures capable of being formed into fibers of high stiffness and strength. Furthermore ,their melt viscosities under processing conditions are often one or two decades lower than that of comparable flexible polymers [4].

Ever since some commercial main chain thermotropic liquid crystalline copolymers were successfully prepared, some of their novel and excellent properties have attracted the attention of scientists and engineers, promoting widespread and profound investigations on the rheological properties, the supermolecular structures and optical textures, as a function of temperature

and the phase transitions in the crystalline, liquid crystalline and isotropic liquid states. Nowadays, much more emphasis in the applications of the thermotropic liquid crystal copolyesters is placed on blending or alloying them with conventional engineering plastics to improve their processability and mechanical properties. An important concept used in the preparation of such blends or alloys is that of the molecular composite, meaning that the semiflexible liquid crystalline macromolecules are molecularly dispersed in conventional plastics and hence the reinforcement takes effect at the molecular level. This concept has promoted investigations of the phase separation processes and the phase-separated structures of blends of liquid crystalline polymers with conventional plastics. Some theoretical studies on the miscibility of polymers take into account the concentration fluctuation and orientation fluctuation in order to describe their phase behaviour [2].

#### **1.1.1.1 Properties of Thermotropic LCPs**

Thermotropic liquid crystalline polymers are well known for their unique mechanical and rheological properties. Due to their rigid molecular structure, they can easily be oriented in the melt by an external field to form a liquid crystalline phase. When processed in the crystalline state, these materials generally possess excellent mechanical properties in the direction of orientation. Furthermore, their melt viscosities under processing conditions (i.e. high deformation and deformation rates) are often lower than that of comparable flexible polymers [5]. Thermotropic LCPs, which are mainly random copolyesters and copolyesteramides, possess a unique combination of

properties. The most significant characteristics are easy precision moldability, high outstanding dimensional stability and chemical resistance, low controllable coefficient of thermal expansion, low flammability and permeability and exceptional strength, stiffness and toughness.

In terms of commercial applications it is interesting to note that three classes of LCPs are emerging. The first is general purpose LCPs that are easy to process. These LCPs possess high dimensional stability, molded-part repeatability, chemical resistance, good flame resistance, high strength and good stiffness. The second class consists of LCPs that are more temperature resistant and not quite as easy to process as the class 1 LCPs, but they have good dimensional stability, good chemical resistance, excellent flame resistance and very good strength and stiffness properties. The third; lower temperature performance class consists of less expensive, less easily processed LCPs, which nevertheless have moderate chemical resistance, moderate flame resistance, good strength and high stiffness.

### **1.1.2 LCP Blends and Effect of LCPs on Morphological Behavior of PET**

Blending of conventional thermoplastics with thermotropic liquid crystalline polymers has attracted much attention over last decade. As its well known, LCPs, existing as ordered domains in the liquid crystalline state, usually exhibit a considerably low melt viscosity and could preferentially be oriented to form fibrils under an elongational flow as encountered in the ordinary melt processing techniques [6].

Blending of thermotropic LCPs with isotropic polymers might result in materials which can be used as an alternative for short fiber reinforced thermoplastic composites or can serve as a matrix material for composites [4].

The properties of the blends are affected by the size, shape and distribution of the LCPs in the matrix polymer, which in turn are related to the processing conditions such as the blend composition, the extrusion and drawing conditions, the viscosity ratio of the component polymers, the type and grade of the LCPs and the matrix polymer. Improved processability of the blend due to the reduction in viscosity and the improved interfacial adhesion between reinforcing fibers and the matrix polymer are among the advantages of these materials over the conventional short fiber reinforced composites.

The potential advantages of in situ composites are that problems occurring during the melt processing of conventional short fiber reinforced composites, such as fiber breakage, wear of the equipment and rise of viscosity, can be avoided. On the contrary, the melt viscosity of the blend would be lowered significantly upon addition of a thermotropic LCP (TLCP). The TLCP, which is initially dispersed as spheres or droplets, can be elongated in adequately strong flow fields to give in situ reinforcement [4].

## **1.2 RECYCLING AND RECYCLED PET**

### **1.2.1 Recycling and Importance of Recycling**

One of the primary factors affecting the mechanical properties of semicrystalline PET polymers is related its crystalline and amorphous regions in the morphological structures. Recent reports on the crystallization kinetics of the PET are focused on engineering grade PET and not on the recycled PET materials. But the investigations proved that all samples containing recycled PET in blends show mechanical improvements with large increases on the elongation as well as impact strength. This is probably due to crystalline morphology and gradients of morphology of the injection molded sample [7].

The enhanced mechanical properties of the recycled PET are explained as a result of the various levels in crystallinity. Because of increased properties of the recycled PET, the recycling of PET became very popular in last years.

The increasing awarness of the environment has contributed to concerns regarding our life styles and our indiscriminate disposal of wastes. The pursuit of a higher quality of life is a continuing goal for the people of this world. This has contributed to the increased consumption of goods and services. A consequence of such consumption is the production of increased pollution and large amount of wastes. The goal of any sustainable growth should be that the efficiency of energy utilization in every step of the

system, from the production of the goods to the disposal of the wastes, be maximized. The interdependence of each of these steps on the others in the total chain necessitates that we address the problems totality [8].

Plastics have become an integral part of our lives. The amounts of plastics consumed annually have been growing steadily (Table 1.1).

Table 1.1 Growth of plastics in MSW in USA [8]

MSW: Municipal solid waste

<b>YEAR</b>	<b>Plastics in MSW ( % )</b>
1960	0.5
1970	2.6
1980	5.0
1990	9.8
1992	10.6
1994	11.2
1995	11.5
1996	12.3

Its low density, strength, user-friendly design and fabrication capabilities and low cost, are the drivers to such growth. Besides its wide use in packaging, automotive and industrial applications, they are extensively used in medical delivery systems, artificial implants and other healthcare

applications, water desalination and removal of bacteria etc. Usage of plastics, in preservations and distribution of food, housing and appliances are too many mention here. Specially designed plastics, have been an integral part the communication and electronics industry, the manufacturing of chips or printed circuit boards, or housing for computers. They are also integral components in the preparation and delivery of alternative energy systems such as fuel cells, batteries and even solar power. The waste plastics collected from the solid wastes stream is a contaminated, assorted mixture of a variety of plastics. This makes their identification, separation and purification, very challenging.

Plastic recycling has grown appreciably during the last few years. Recycling of rigid plastic containers has grown to about 649 million kg. of waste PET bottles in 1997. A major problem faced by the plastics industry is that of waste proposal [8]. Recycling material would appear to offer a solution which is satisfactory in terms of preventing environmental pollution. Increasing interest has recently, been focused on the recycling of plastic wastes, especially PET scrap [8].

PET is already being recycled and a number of uses have been found for it, including: fibrefill, fabric, automotive parts, industrial strapping, sheet and film, new containers for both food and non-food products, containers for baked foods [9].

From this wide variety of regenerated materials, numerous applications for recycled polyesters can be explored depending on the properties of the resin as well as the additives used (impact modifiers, mineral fillers ,glass fibers,etc.) to upgrade the material [9].

In the plastics waste stream, polyethylene forms the largest fraction which is followed by PP, PVC and PET.

A common problem faced during processing of recycled PET is hydrolysis, which reduces its average molecular weight. Thermal exposure, as well as shear degradation, will also lead to molecular weight loss. These losses will result in plastic material with reduced melt viscosity, impact resistance and mechanical properties.

There are three main factors, which must be considered regarding the issue of recycling: first, collection of the waste; second, recycling process itself; and third whether or not there is a market for the end product of recycling. The third factor is of course the most important.

Recycling PET gives rise to a decrease in the melt viscosity, average molecular weight, thermal and mechanical properties of the material because of the hydrolytic chain scission and thermomechanical degradation undergone during processing. The studies done for crystallization of recycled PET shows that recycled PET is as good as any engineering grade plastics, if not better, for some applications, because of the easy crystallization and processing. PET wastes are potential source for recycling applications. PET recycling has become common in the industry. Different processes are available for the recycling [8].

### 1.2.2 Methods And Uses For Recycling PET

Different processes are available and most of them consist of esterifying the polyester with an excess of reactant such as diols, diamines, alcohols or water. PET conversion products are used as monomers for further synthesis of PET, polyurethanes or polyesters. Table 1.2 summarizes the most popular methods to treat PET wastes [10].

Table 1.2 Most Popular PET Waste Treatment Methods

TREATMENT	REACTANT	REACTION PRODUCTS
Alcoholysis	EG	BHET and EG
Hydrolysis	Water	Terephthalic acid and EG
Aminolysis	Amine	Terephthalamide
Methanolysis	Methanol	Dimethyl terephthalate and EG

The recovered PET material from beverage bottles has formed many applications, from the use of engineering PET to out door well-worn hiking boots, rugged sweaters, and most garments made of polyester. The blending of virgin PET and recycled PET has been the worldwide trend in many applications.

## **1.3 PET AND LCP BLENDS**

### **1.3.1 Fibrillation**

PET is a semi-crystalline polymer that is widely used for synthetic fibers because of its excellent properties. Further improvement in the PET fiber properties can be accomplished by chemical modifications or by blending with other polymers. In general fiber's mechanical properties are improved by blending it; with a liquid crystalline polymer [11].

Fibrillation occurs only under special conditions that are dependent on rheological parameters such as deformation rate and viscoelastic properties of the matrix as well as on the polymer-polymer interaction in the blend [11].

### **1.3.2 Fibers from Liquid Crystalline Polymers**

Fibers made from liquid crystalline polymers are particularly attractive for two reasons. First, the fibers show excellent mechanical properties and thermal and thermooxidative stability. Second, the fibers can be spun in the low ordered liquid crystalline states where the substantially reduced viscosity leads to better processability during fiber spinning. We focus on the anisotropic rheological properties of liquid crystalline polymers which are important features in the understanding and application of the unique molecular and supra-molecular structures of these materials. It is well-known

that liquid crystalline polymers exhibit low viscosities compared with isotropic fluids. This has been explained as a result of very efficient molecular orientation fields, in particular, at high strain rates [12-15].

The strongest motivation for exploring liquid crystalline polymer fibers came from their applications in high-performance composite materials, specifically in the aerospace industry. The rapid development of this field generated a need for novel liquid crystalline fibers with improved properties and reduced weight [16].

The basic technology for forming synthetic fibers includes spinning and heat treatment using different drawing methods. To spin fibers from low ordered liquid crystalline states, it is important to distinguish lyotropic and thermotropic systems, although both of them have the advantages of relatively low viscosity, which improves processability. Fibers spun from lyotropic liquid crystalline polymers usually employ a wet or dry-jet wet spinning method (sometimes, gel spinning for high molecular weight or rod-like polymers may also be feasible), while those spun from thermotropic liquid crystalline polymers use a melt spinning method. The wet spinning process, so called because aqueous solutions are often used as coagulating agents, is employed mostly for lyotropic liquid crystalline polymers in nonvolatile solvents. The extrudate is immersed directly in a non-solvent bath, where fiber coagulation and solution extraction take place. A combination of wet and dry spinning methods, so called dry-jet wet spinning, is extremely useful in fiber formation from lyotropic liquid crystalline polymers. In this process, the polymer solution is passed through a short air gap prior to immersion in the coagulation bath. This prevents the solution from freezing inside the

spinnerette. In fact, most high strength and high modulus synthetic fibers are spun using this method.

For thermotropic liquid crystalline polymers, a melt spinning method is adopted to produce fibers. The anisotropic polymer melt is expelled from small capillary holes to form fibers which are attenuated by an external force, and then cooled into the solid state. The majority of the molecular alignment is developed by extensional flow during drawdown immediately after spinning from the low ordered liquid crystalline melt. At shear rates experienced during the fiber spinning, on the order of  $10^3$  to  $10^4$   $\text{s}^{-1}$ , the viscosity of a thermotropic copolyester, for example, lies between  $10^1$  and  $10^2$   $\text{Nsm}^{-2}$ . The marked shear thinning of the liquid crystalline melt can be seen as an important contribution to the low viscosity at these high shear rates. Furthermore, the viscosity is also dependent upon molecular weight. Melt spinning is also possible for fibers spun from the isotropic melt at even higher temperatures. However, this process loses the advantage of the relatively low viscosity during fiber spinning. Therefore, in this fiber spinning process, the temperature and external force distribution along the spinning line are the two key factors which affect the performance of the fibers.

Following spinning, a fiber is heat treated by one of three methods: (1) free-end annealing, (2) fixed-end annealing, or (3) annealing under extension. Generally, the heat treatment is applied to improve the fiber strength and/or modulus. Sometimes, a zone-annealing method is also used [17]. The method used varies from fiber to fiber, depending on the application. From a molecular point of view, the various spinning methods and heat treatment processes affect the chain orientation, crystallinity, crystal size and morphology in the fibers.

The molecular mechanism in the spinning and heat treatment that leads to chain alignment and crystallinity have several major components: rheological behaviour of liquid crystalline polymers in the anisotropic melt or solution under shear flow in the spinnerette hole, elastic relaxation of the liquid at the capillary exit, elongational flow along the fiber axis before solidification and crystallization upon cooling or coagulation of the fibers. The ideal case would be two step fiber formation process, namely, a polymer fluid which would allow the uniaxial orientation, the molecules could then crystallize extremely quickly in order to solidfy the fibers. The design of fiber spinning for liquid crystalline polymers is an attempt to rationally approach this ideal case. One approach would be to utilize the concept of monotropic liquid crystalline behaviour to form fibers. If one could design a liquid crystalline polymer which exhibits monotropic behaviour and has an extremely slow crystallization rate or needs an external force field to induce crystallization, one might then spin fibers at relatively low temperatures (lower than melting temperature) in the liquid crystalline state. The resulting fibers could then be crystallized during annealing under an external force field. All of the aspects associated with the process require a broad knowledge of polymer physics, chemistry and processing technology. Basic structural parameters in fibers are usually characterized by various analytical methods during each step of the fiber formation. In addition, macroscopic thermal, chemical and mechanical properties can be measured. However, the establishment of relationships between structure, properties and processing conditions in high performance fibers obtained from liquid crystalline polymers is still not complete.

It should be pointed out that the properties of synthetic fibers spun from the liquid crystalline (either lyotropic or thermotropic) are more critically dependent upon the fiber spinning process than those prepared using common fiber formation processes. This is because during fiber spinning, the anisotropic fluid is uniaxially orientated relatively easily and the fiber structure has formed, it is difficult to completely change the structure and develop new structure during the heat treatment process. Therefore, heat treatment can only improve the existing structure in order to enhance mechanical performance. This understanding can be supported by experimental observations that heat treatment causes an improvement in modulus but has little effect on strength in many high performance fibers spun from the liquid crystalline state [18].

### **1.3.3 HBA / PET Copolyester Fiber Structure, Morphology and Properties**

The copolymers of hydroxy benzoic acid (HBA)/PET were first developed by Eastman Chemical Company under the trade name X7G. Although this series of copolyesters have random composition sequences, it was later determined that the two components are more or less phase separated by using several experimental methods. This biphasic morphology certainly affects the fiber structure and properties. When the fibers were spun at relatively low temperatures, a domain structure of randomly oriented crystallites were observed, while in fibers spun at high temperatures a well-developed fibrillar structure was found. WAXD results showed that molecular orientation increased with increasing processing temperature. Although it is

generally agreed that the biphasic structure is an indication of microphase separation of the two components in HBA/PET copolyesters, there is still a great deal of discussion regarding the sequence of randomness or blockiness in the copolyesters. This must be associated with monomer compositions, polymerization conditions, as well as thermal and external force field histories of the polymers during fiber spinning.

Most HBA/PET copolyester fibers exhibit moderate tensile moduli. The highest was around 32 GPa. However, the tensile strength at break was very low (less than 0.3 GPa). This is possibly due to the low molecular weight of the copolymers used in the investigation. These data were obtained for 60/40 PABA/PET fibers oriented at 225°C. It was reported that [18] the take-up speed of fiber spinning as well as the heat treatment were very important in determining the ultimate mechanical properties. Recently, it was found that the tensile properties of these copolyester fibers could be improved by various annealing processes [18]. However, the thermal behaviour of as-spun and heat treated copolyester fibers showed thermal transition behaviour which was similar to that of the bulk samples [18].

In this work X7G (40% PET /60% PABA) was used as a copolyester (Figure 1.1).

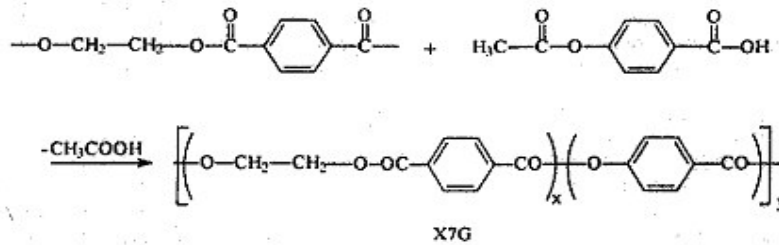


Figure 1.1 Structure of X7G copolyester

### 1.3.4 Wind Up Speed Suppression (WUSS) Effect

It has been reported [19-21] that interesting and useful changes in fiber properties can result from immiscible polymers added to melt spinning. In particular, at a given take-up speed, molecular orientation in the melt-spun fibers is substantially reduced.

Since orientation increases with wind-up speed, the resulting blend fiber has properties resembling those of one-component fibers spun at lower wind up speed. Harry Brody [19] named this effect 'wind-up speed suppression' (WUSS).

For example, birefringence of PET fibers containing 3% of a copolymer of 6-oxy-2-naphthalene and paraoxybenzene spun at WUS of 4000 m/min was the same as for pure PET spun at 2400 m/min [19].

Till now the WUSS effect was observed in PET, nylon 66, polypropylene and polyethylene fibers with various additives [19-22]. Two groups of these additives can be distinguished: thermotropic liquid crystal polymers (LCP) and non-crystal polymers (non LCP). LCPs are specially effective in suppressing orientation for different threadline temperatures. Non-LCP additives need activation by cooling the threadline.

For example, PET blended with 3% of polyethylene spun at 300<sup>0</sup>C shows no reduction of orientation when the throughput per spinneret hole was 98 g/h, but WUSS was evident when the throughput was reduced to 40 g/h [19].

The possibility of spinning low oriented fibers at high wind-up speeds is very important from the commercial point of view. It leads to increased productivity of melt spinning process. This is so because the draw ratio required for predetermined final thickness is increased by reduced orientation and filaments with larger undrawn diameter can be spun [3].

#### **1.4 Scope of Work**

In this work our basic aim is to obtain a continuous or discontinuous fiber from liquid crystalline copolyester, X7G, and recycled PET blend. For this purpose a comparative study of the forementioned blend and fiber grade and bottle grade PET is initiated. Their thermal, mechanical and fiber forming properties are studied to understand the conditions under which an economical and value-added product can be produced from recycled PET.

## CHAPTER 2

### EXPERIMENTAL

#### 2.1 MATERIALS

The virgin polyethylene terephthalate samples (fiber grade and bottle grade) were kindly supplied by SASA A.Ş. The recycled polyethylene terephthalate sample was obtained from Geç Kimya, Gaziantep. The liquid crystalline copolyester X7G which is 60% paraacetoxybenzoic acid and 40% PET (60%PABA/40%PET) was synthesized in our laboratories[22]. Trifluoroacetic acid/dichloromethane was used as a solvent in solution viscosity measurements. Trifluoroacetic acid was purchased from Aldrich Chemical Co. while dichloromethane was from Carlo Erba. Both were used without further purification.

#### 2.2 Synthesis of X7G

In this procedure polymers were prepared, without added catalyst, from equimolar amounts of PABA with the required amount of PET. The hydroxyl group in HBA is reduced by acetyl group for ease of reaction. Dry monomers weighed to an accuracy of  $\pm 1$  mg on a sheet of aluminum foil were placed in a glass polymerization reactor (diameter 3.6 cm, length 22 cm) (Fig.2.1).

The system was purged 5 times with nitrogen in all cases about half an hour and then heated at 250<sup>0</sup>C rapidly by immersing the reactor into the preheated solder bath. The reactants were melted under the continuous flow of dry and clean nitrogen. While they were stirred in a nitrogen atmosphere, acetic acid as a by-product of the polycondensation was distilled out and collected volumetrically. At this stage of the reaction, a clear solution was observed. When the collected amount of acetic acid remained constant, water condenser was taken off from the system. Then the temperature of the reaction medium was raised to 290-300<sup>0</sup>C quickly and polymerization was continued in the melt phase. Entire mixture started to become turbid. After obtaining a low melt viscosity (about 45 min.) vacuum was applied gradually by first closing by-product outlet valve and then feeding nitrogen only through the restricting capillary route for 15 min. Thereafter 0.5 mmHg vacuum was introduced to the system after cutting off the nitrogen supply completely and held for 3 hours at 290<sup>0</sup>C under vacuum. During all copolyester synthesis a finishing temperature of 290<sup>0</sup>C was used, as undesirable side reactions leading to chain branching and cross-linking had taken place at higher temperature.

After 3 hours period, vacuum was broken by allowing the nitrogen flow inside and under a nitrogen blanket the reactor was taken off from the still-head. During quenching, the tube was circulated inside the liquid nitrogen. The polymer was taken out by breaking the glass reactor and dried under vacuum at 80<sup>0</sup>C overnight [22].

### **2.3 Preparation of PET and LCP (X7G) Blends**

A large tube is used for the blending process. The tube is 25-30 cm in length and has a 30 mm inner diameter. The blend is mixed under nitrogen atmosphere and in the silicon oil bath at a set temperature of 275°C. The schematic diagram of the reactor is given in Figure 2.1.

Firstly, the bath is allowed to reach the set temperature and then the tube is inserted into the silicon oil bath. A spiral mixer (Figure 2.2) was used to obtain homogeneous mixture. After 30 minutes the blend is taken from the silicon oil bath and allowed to cool at room temperature, after cooling, the tube is broken to recover the blend. During this process a certain amount of trans-esterification, ester exchange chain elongation reactions can be expected which can result in the incorporation of liquid crystalline moiety into the PET polymer chain.

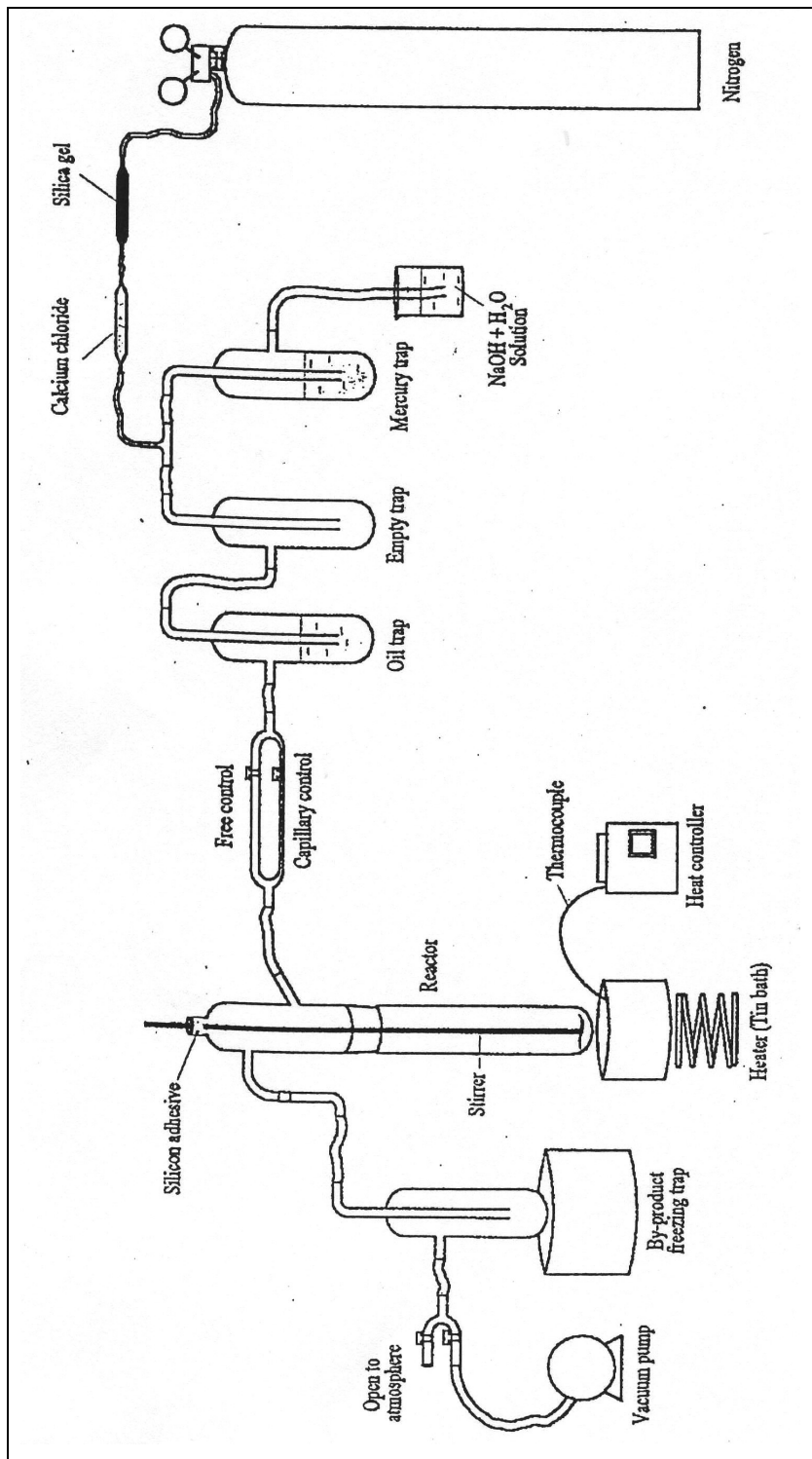


Figure 2.1 Polymerization and Blending System



Figure 2.2 Spiral mixing head of the Reactor.

## **2.4 FIBER FORMATION PROCESS**

### **2.4.1 Fiber Spinning**

We used a simple fiber spinning machine designed by Bedii Erdemir and Merih Şengönül [22] (Figure 2.3). The apparatus has a maximum capacity of 50 g polymer. The spinnerets were supplied by SASA A.Ş. and the other parts are constructed in the machine shop. Melt spinning is performed using the extruder with capillary length of 0.060 inch, diameter of 0.020 inch so that the ratio of  $L/D$  is 3. The extruder consists of a heating block which houses the melter barrel and can be pushed down the barrel with  $10 \text{ kg/cm}^2$  pressure of nitrogen gas. The barrel of the melter unit is 100 mm long and has 26 mm inner diameter and requires a minimum 15 g polymer charge. A filter pack which is sealed by aluminum gaskets to prevent leakages is situated below the melt block in the lower part of the barrel.

The melter unit is assembled outside and then inserted into the heater barrel where it is held in place by a thrust ring at the bottom. The inner diameter of the barrel was 36 mm. The heater barrel is equipped with two ring resistance heaters, each has 100 W power. The isothermal chamber had a length of 90 mm and is isolated from surrounding with a thick glass fiber blanket. The extrusion temperature was controlled by a thermocouple that approaches to the melting chamber until 2 mm distance is left.

The maximum temperature attainable for both the barrel and the pack is 450°C. About 18 g of polymer was used for each extrusion. In order to avoid the absorption of moisture, the polymer granules were charged into the melter barrel under a blanket of nitrogen at a temperature 10°C above the spinning temperature for the purpose of compensating the heat loss during charging. The charge is waited at the spinning temperature under nitrogen atmosphere at about 15 min. to ensure thermal equilibrium. After that, the polymer was melted and forced from a cylinder-piston through a sand bed into the spinneret via a wire gauze. The molten polymer is filtered by passage through a layer of alumina and two layers of stainless steel screens, one fine mesh screen at the top and one coarse mesh screen at the bottom. The screens are incorporated into an aluminum ring, which behaves as a gasket. The spinneret is positioned just below the screens and is retained in place by the spinneret cap. While the spinneret is fitted tightly with spinneret cap to its place, the soft aluminum gaskets deform due to pressure so that there is an intimate contact between the surfaces through which leakage can occur.

The filaments that are spun vertically downwards in air were cooled at room temperature and collected on a 15 cm diameter bobbin placed at a

distance of 100 cm from the die exit. The draw ratio, defined by Dibenedetto, is the ratio of the cross-sectional area of the die to that of the final fiber. Die swell was assumed to be negligible, so the diameter of the spinneret is taken as 0.03 inch that is 0.508 mm.

The diameter of the final fiber was determined using Olympus microscope. The spin draw ratio can be adjusting the speed of the take-up rollers. For this reason the winding speed of the motor head was adjust by a Servosan AC01 0.75 kW AC motor speed controller. The winding speed was infinitely variable between 0 to 1300 m/min. It is kept at 150 m/min for all spinning experiments. These speeds can be considered as low when compared to commercial fiber spinning.

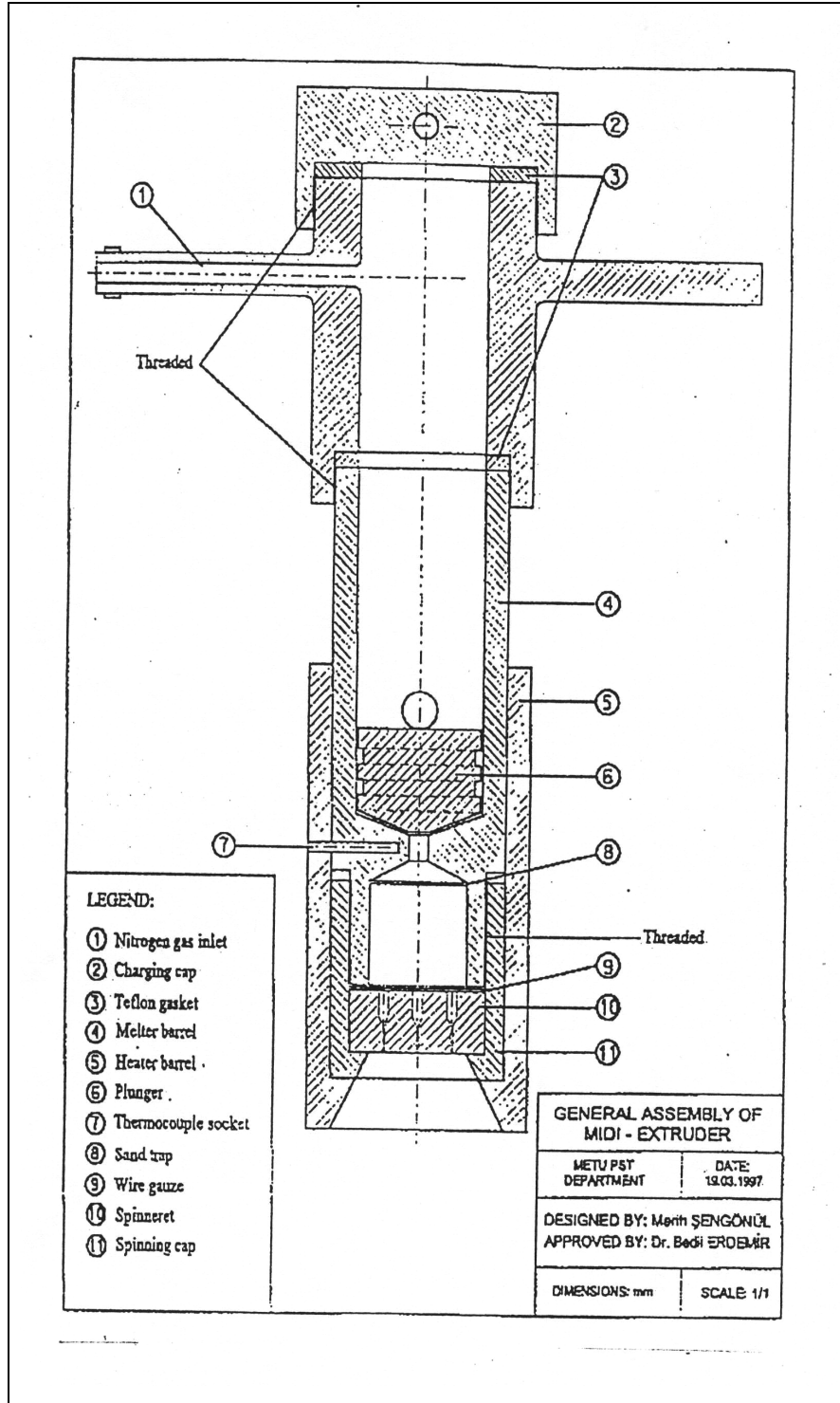


Figure 2.3 Engineering Drawing of Midi - Melt Extruder

## 2.5 DRAWING PROCESS

Drawing process is the last step for fiber spinning. The process increases the crystallinity of the fibers and makes the fibers more orientated. Also the process improves the mechanical properties of the fibers.

Because of the lack of a drawing instrument, a Gallenkamp tube oven (Figure 2.4 ) and a hand made fiber holder system (Figure 2.5 ) was used for this process.



Figure 2.4 Drawing System



Figure 2.5 Fiber Holder

The tube is brought to the set temperature and fiber holder system is inserted into the tube. After allowing for the thermal equilibrium the fibers are extended manually to the predetermined draw ratio.

## 2.6 CHARACTERIZATION METHODS

### 2.6.1 Melt Flow Index Measurements

The melt flow index is not an intrinsic or fundamental property of a polymer. It is rather a convenient property of a polymer for estimating processing and flow characteristics. The melt index, also known as melt flow rate, measures the rate of extrusion of a thermoplastic material through an orifice of standard diameter under prescribed conditions of temperature and load. The weight of the material extruded during the specified time is the melt index expressed in grams per ten minutes [23].

The melt flow index (MFI) measurements were done at 260°C and with a load of 2.16 kg in Coesfeld meltfixer (Figure 2.6). The amount of polymer extruded through a standart die in grams per 10 minutes is called the MFI value of the polymer.



Figure 2.6. Melt Flow Index Instrument

## 2.6.2 Solution Viscosity Measurements

Solution viscosities of polymers were measured in 30/70 (v/v) mixture of trifluoroacetic acid and dichloromethane at 25<sup>0</sup>C.

Solution viscosity measurements were done by using a Cannon E212 type Ubbelohde capillary viscometer. Constant temperature was maintained by using a thermostated water bath fixed at 25<sup>0</sup>C. The polymer solutions (concentrations 0.5 g/dl) were prepared at room temperature by shaking the flasks containing the polymer and the solvent up to 24 hours. Polymer solutions were then diluted in the viscometer by adding 3 ml of solvent. The solution was mixed thoroughly and slowly by passing air from it and the system was kept for 5 minutes to reach the equilibrium and flow times were measured.

All viscosity measurements were performed triple. First, the flow time of solvent was measured. The flow time of solvent is high enough to ignore the Hagenbach-Coutte corrections.

The relative viscosities,  $\eta_r = t/t_0$  were measured; where  $t$  and  $t_0$  are the flow times for the solution and solvent respectively. The intrinsic viscosity  $[\eta]$  is obtained from the reduced viscosity  $\eta_{red}$  and inherent viscosity  $\eta_{inh}$  versus concentration plots by extrapolation to zero concentration [24].

The reduced viscosity and the inherent viscosity are described by the Huggins and Kraemer equations respectively:

$$\eta_{sp}/C = [\eta] + K'[\eta]^2C \quad (1)$$

$$\ln\eta_r/C = [\eta] - K''[\eta]^2C \quad (2)$$

where;

$\eta_{sp}$  is the specific viscosity and  $\eta_{sp} = \eta_r - 1$

$\eta_{inh}$  is the inherent viscosity

$\eta_r$  is the relative viscosity

C is the concentration (g/dl)

$[\eta]$  is the intrinsic viscosity (dl/g)

K' is the Huggins constant

K'' is the Kraemer constant

The Huggins and Kraemer constants are related as shown below:

$$K' - K'' = 0.5 \quad (3)$$

If  $K' - K'' = 0.5$  condition is satisfied, the intrinsic viscosities can be calculated from single point measurements using the following equation which is the algebraic difference of the above equations:

$$[\eta] = \sqrt{2} / C (\eta_{sp} - \ln\eta_r)^{1/2} \quad (4)$$

The Huggins and Kraemer equations provide the most common procedure for evaluation of  $[\eta]$  from experimental data. This involves a dual extrapolation according to these equations and gives  $[\eta]$  as the mean intercept of the lines of both equations. The intrinsic viscosities were obtained from the mean intercepts.

### 2.6.3 Differential Scanning Calorimetry

Differential scanning calorimetry (DSC) is the most widely used thermal analysis technique. Differential scanning calorimetry is the standard technique used for measuring transition temperature and also enthalpy changes at these transitions. In DSC, the heat flow into or away from a reference is measured as a function of temperature or time.

Calorimetric measurements were performed using a Dupont (910S.V4.1) differential scanning calorimeter. The DSC cell was calibrated for temperature and enthalpy response to the melting points and heats of fusion of pure indium metal [24].

The basic equipment consists of two aluminum pans, one a reference pan, the other containing a few milligrams of the material to be tested. Polymer samples weighing between 5-8 mg were placed in closed aluminum pans. Heat is supplied to the pans so that their temperatures were maintained equal as the temperature raised. The samples were scanned between 25–300°C at a rate of 10°C /min under nitrogen atmosphere during first run.

#### **2.6.4 Scanning Electron Microscopy**

A well-known method for examining surface detail is scanning electron microscopy. The scanning electron microscope is a microscope that uses electrons rather than light to form an image. The combination of higher magnification, larger depth of focus, greater resolution and ease of sample observation makes the SEM one of the most widely used instruments in research areas today. By scanning an electron cascade across a specimen, high resolution 3D images of morphology with high magnifications can be obtained. The main use of scanning electron microscope in fiber science has been in the range of medium to high magnification, which is near or beyond the limit of the optical microscope [25].

A scanning electron microscope JEOL JSM-6400 was used to investigate the fracture morphology and structure of the PET-LCP fibers. The SEM studies were done on surface coated samples.

#### **2.6.5 Fiber Tensile Test**

Tensile test in a broad sense is a measurement of the ability of a material to withstand forces that tend to pull it apart and to determine to what extent the material stretches before breaking. Tensile properties of the fibers were measured on a Lloyd LS 500 tensile testing machine at room temperature. The sample is clamped at one end and pulled at a constant rate of elongation until the center of the specimen fails. The load vs. extension curves

were obtained. The diameter of each filament was measured directly by an Olympus microscope equipped with a calibrated eyepiece scale [25].

A thin paper or a cardboard, compliant metal or plastic strip with a longitudinal slot of fixed gage length can be used as a mounting tab for the single filament.

The mounting tab (Figure 2.7) should be as thin as possible to minimize filament misalignment. During this work very thin cardboard is preferred for this reason.

The load-sensing device should have sufficient capacity to accept and transmit load signals above the highest anticipated loads. Therefore during the experiments, the 10N load cell which has the lowest load determining capacity available at the test facility was used.

A random selection of single filaments is made from the material to be tested. The filaments are center-line mounted on pre-cut cardboard frames. The frames are gripped so that the test specimen is aligned axially in the jaws of a constant speed movable crosshead test machine. With the frame unstrained, both sides of the frame are cut very carefully.

The fibers were tested with a gauge length of 20 mm and an extension rate of 2 mm/min. Tests were carried out five to ten times for each sample.

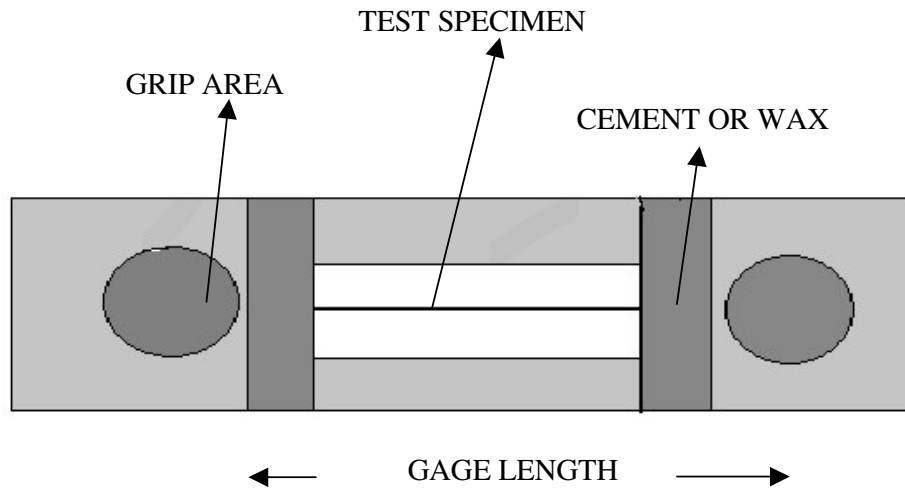


Figure 2.7 Single Fiber Specimen Mounting Set-up

### 2.6.6 Wide Angle X- Ray Diffraction (WAXD) Analysis

X-Rays are electromagnetic radiation with typical photon energies in the range of 100eV-100keV. Because the wavelength of X-rays is comparable to the size of atoms, they are ideally suited for probing the structural arrangement of atoms and molecules in a wide range of materials [26]. The energetic X-rays can penetrate deep into the materials and provide generally by X-Ray tubes. The Rigaku Miniflex (Cu,  $K\alpha$ , 30 kV, 15 mA ) instrument was used for X-ray diffraction analysis.

Because of the need of a compact powder sample in the instrument, the fibers were cut into small pieces which proved to be unsatisfactory. The required compaction could not be achieved by this technique. We next tried to powderize the fibers by freezing in liquid nitrogen and crushing in a marble bowl manually. This technique also did not give a totally satisfactory compaction of the material in powder form.

## CHAPTER 3

### RESULTS AND DISCUSSION

#### 3.1 Melt Flow Index Results

The results of melt flow index measurements carried out on PET and PET/LCP blends are given in Table 3.1. It is apparent that the heat treatment in the first run causes an increase in the viscosities of all samples except one sample containing bottle grade PET(BGPET)+1%LCP blend. This can be attributed to an increase in the molecular weight.

The other observation is the effect of the liquid crystalline polymer addition on the melt flow index values. Compared to the same samples without LCP component; melt flow values increase with LCP addition indicative of a decreases in absolute viscosity values in the first runs. This is an expected result since the rigid rod LCP component acts as flow regulators by aligning along the flow lines. As LCP content is increased to 2% in the recycled samples MFI value increases slightly in the first run and again slightly larger in the second run indicating an orientation effect.

Another important result is that the second heat treatment normalizes the flow regime with MFI values in a narrow regime between 6.4 and 8.2. The first run on the other hand, show large fluctuation between 10 and 60. It is

also interesting that the 1%LCP added recycled PET (R-PET) has an optimum MFI value for fiber formation.

Table 3.1 Melt Flow Index Values of PET and PET-LCP Blends

( 260 <sup>0</sup> C ; 2,16 kg )	FIRST RUN (g/10min)	SECOND RUN (g/10 min)
BGPET	14.8	7.4
BGPET + 1% LCP Blend	41.0	very high
BGPET + 2% LCP Blend	61.5	6.8
FGPET	20.8	6.4
R-PET	10.5	7.2
R-PET + 1% LCP Blend	19.8	6.8
R-PET + 2% LCP Blend	21.0	8.2

It should be remembered that bottle grade PET (BGPET) has a higher molecular weight compared to fiber grade PET (FGPET) and it also has a small amount of isophthalic acid comonomer besides the main component terephthalic acid to repress crystallization. The results of the BGPET+1% LCP is curious indicating the complex rheological character of LCP containing blends [19,32,34].

### 3.2 Solution Viscosity Results

Trifluoroacetic acid and dichloromethane mixture was used as a solvent as mentioned in the experimental part. As expected the BGPET has the highest intrinsic viscosity (Table 3.2). The X7G was shown to have very low intrinsic viscosities (around 0.16) in previous work [27], therefore, the blends have lower values compared to unblended samples. It is interesting to note that the R-PET and LCP blended R-PET have similar intrinsic viscosities to that of common fiber grade PET, which is around 6.8, and based on this knowledge alone they look to be spinnable. Of course, spinnability depends on other factors such as regularity of the molecular structure, interchain interactions besides intrinsic viscosity.

Table 3.2 Intrinsic Viscosity Results of the Bottle Grade PET, Recycled PET and their Blends with LCP

	BGPET	BGPET+ 1%LCP Blend	BGPET + 2% LCP Blend	R-PET	R-PET+ 1%LCP Blend
Intrinsic Viscosities [ $\eta$ ]	0.78	0.52	0.50	0.69	0.67

### 3.3 DSC Results

Thermal behaviour of the various PET and PET blends are given in the following figures. The crystallization temperature ( $T_{\text{cry}}$ ) and the melting temperature ( $T_{\text{m}}$ ) of all the samples are given in Table 3.3. The FG PET shows a typical behaviour with the exothermic crystallization peak around  $130^{\circ}\text{C}$  and the melting endotherm at about  $251^{\circ}\text{C}$  in Figure 3.1. The spun fiber of the same material shows similar behaviour that indicates the crystallization process during spinning is not complete for the air quenched fiber. The melting temperature is even lower by  $2^{\circ}\text{C}$  compared to PET chips (Fig.3.2a). The drawn sample of the fiber grade spun fiber is given in Figure 3.2b. The crystallization peak in the DSC thermogram does not exist in this case which shows that some amount of crystallization is achieved in the drawing process. Also, the melting temperature has slightly increased to over  $250^{\circ}\text{C}$  from  $249^{\circ}\text{C}$  due to the drawing process.

The thermogram of the BG PET in Figure 3.3 is interesting. It has no crystallization peak due to the annealing process carried out during production and also it shows two minima one being at rather low temperature of  $238^{\circ}\text{C}$  and the other smaller one at  $251^{\circ}\text{C}$ . This is perhaps due to the isophthalic acid moiety that changes the crystal morphology and crystallite sizes for the one at  $239^{\circ}\text{C}$  and the one at  $251^{\circ}\text{C}$  is the regular PET melting peak.

Table 3.3  $T_{\text{cry}}$  and  $T_{\text{m}}$  values of the Samples

	$T_{\text{cry}}$ ( $^{\circ}\text{C}$ )	$T_{\text{m}}$ ( $^{\circ}\text{C}$ )
FGPET	129.38	251.74
Spun FGPET	130.43	249.69
Drawn FGPET	-----	250.41
BGPET	-----	238.35
Spun BGPET	127.88	252.38
BGPET +1%LCP Blend	-----	249.83
BGPET +2%LCP Blend	-----	248.93
R-PET	-----	247.20
R-PET +1%LCP Blend	-----	249.30
R-PET +2%LCP Blend	-----	248.90

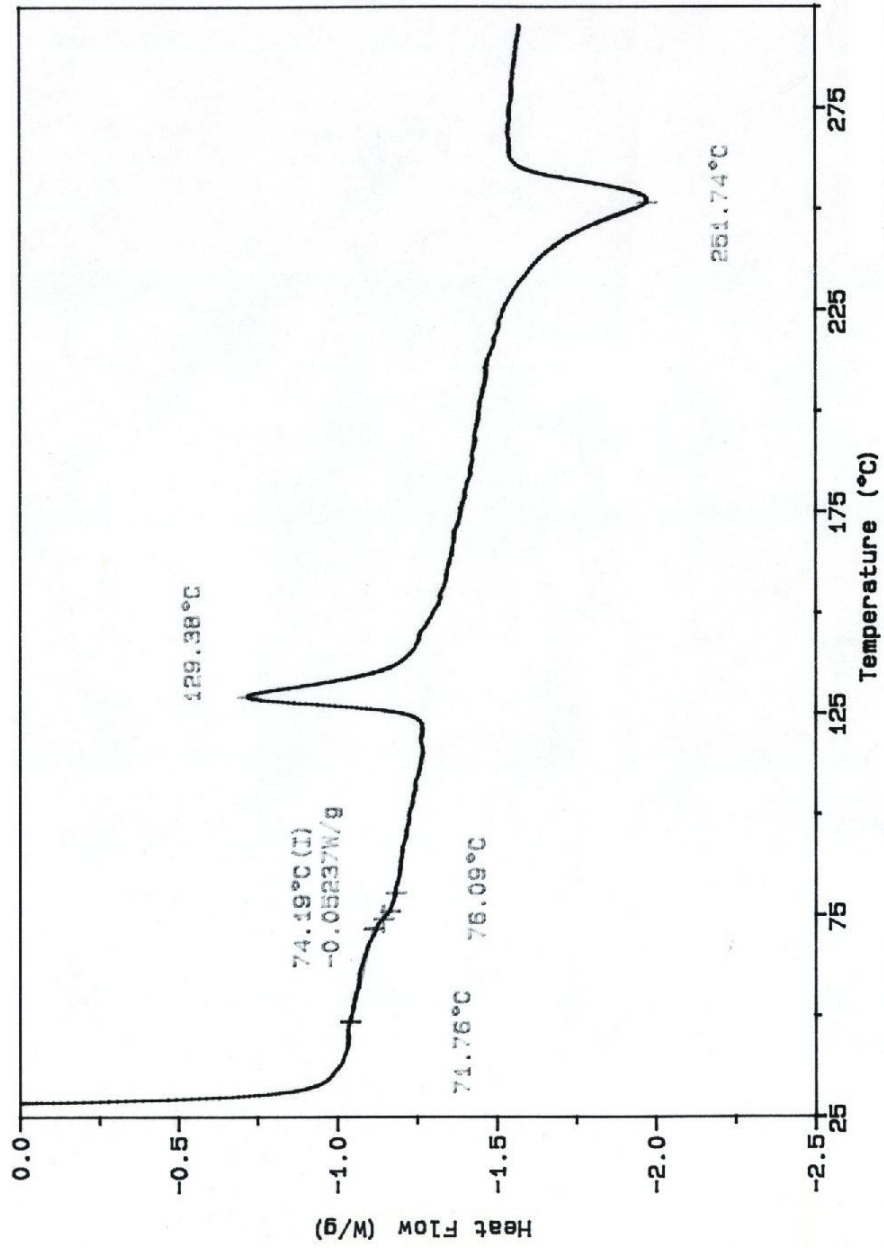


Figure 3.1 DSC Thermogram of Fiber Grade PET (FGPET)

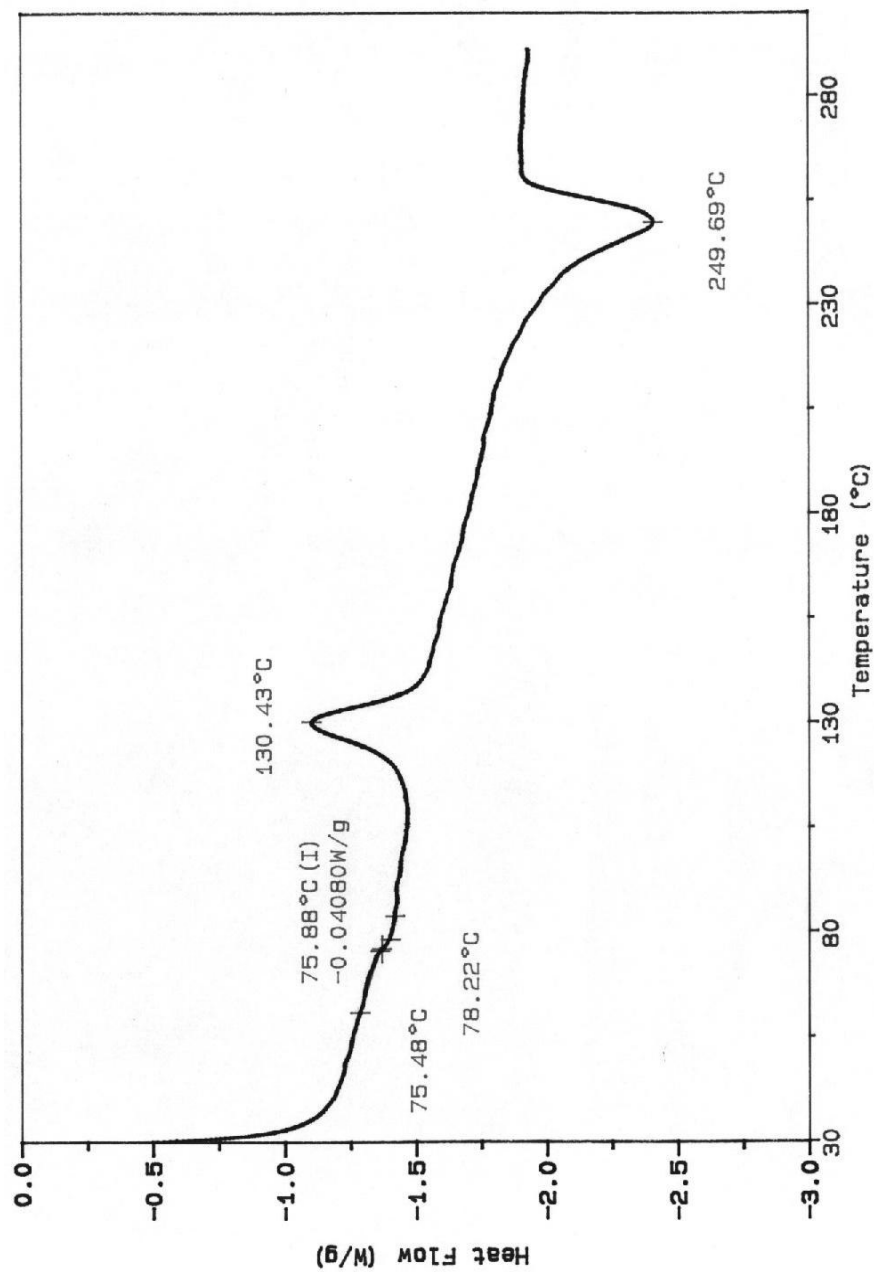


Figure 3.2a DSC Thermogram of Spun Fiber from FGPET

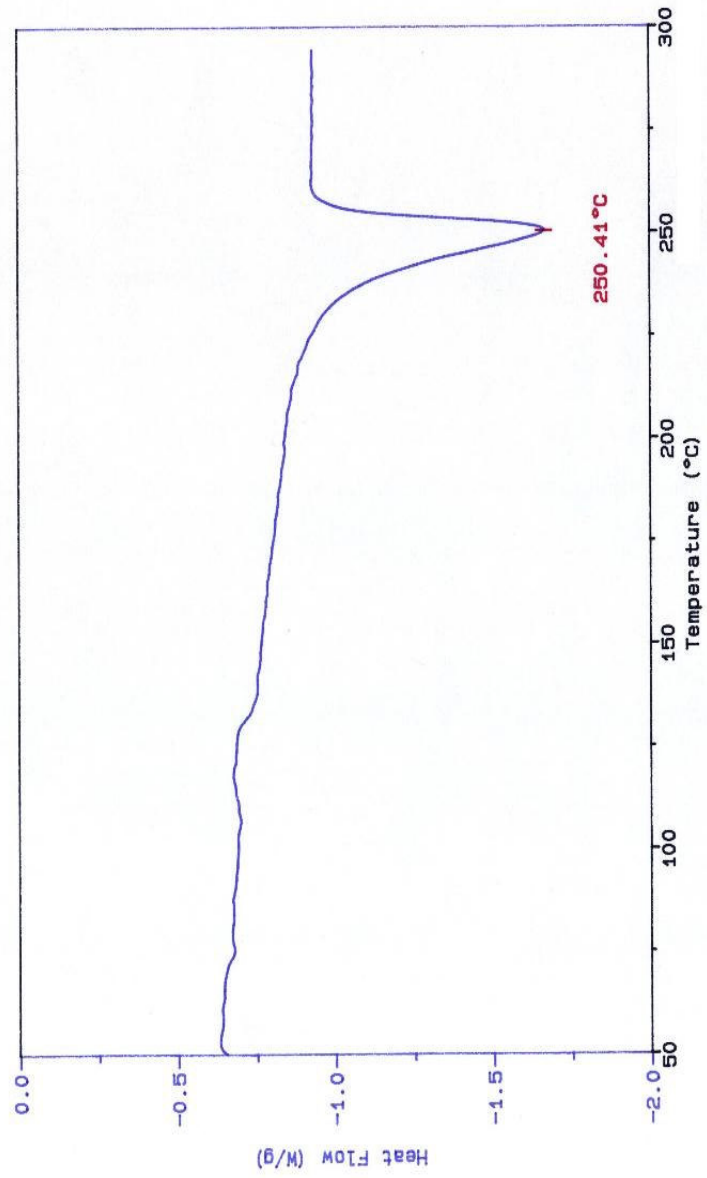


Figure 3.2b DSC Thermogram of Drawn Fiber from FGPEt

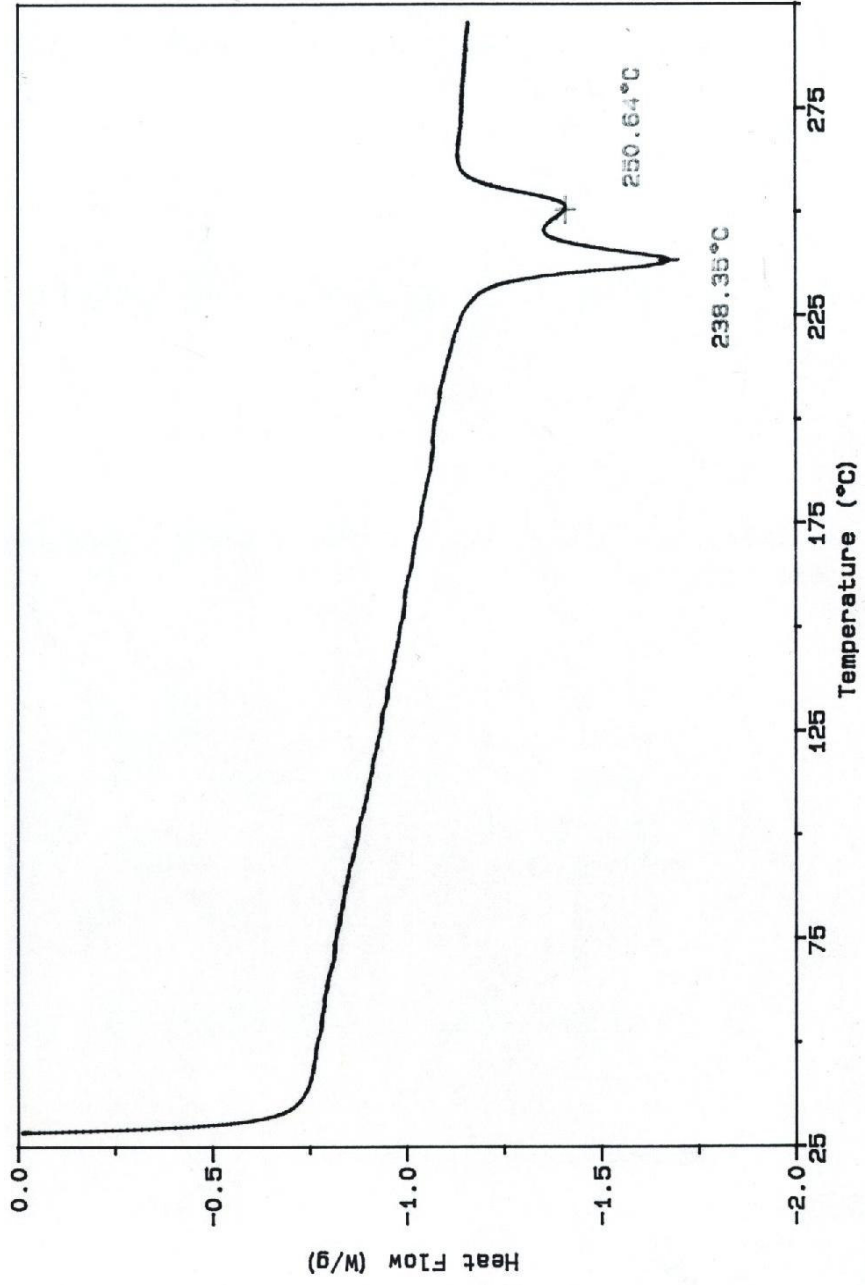


Figure 3.3 DSC Thermogram of Bottle Grade PET (BGPET)

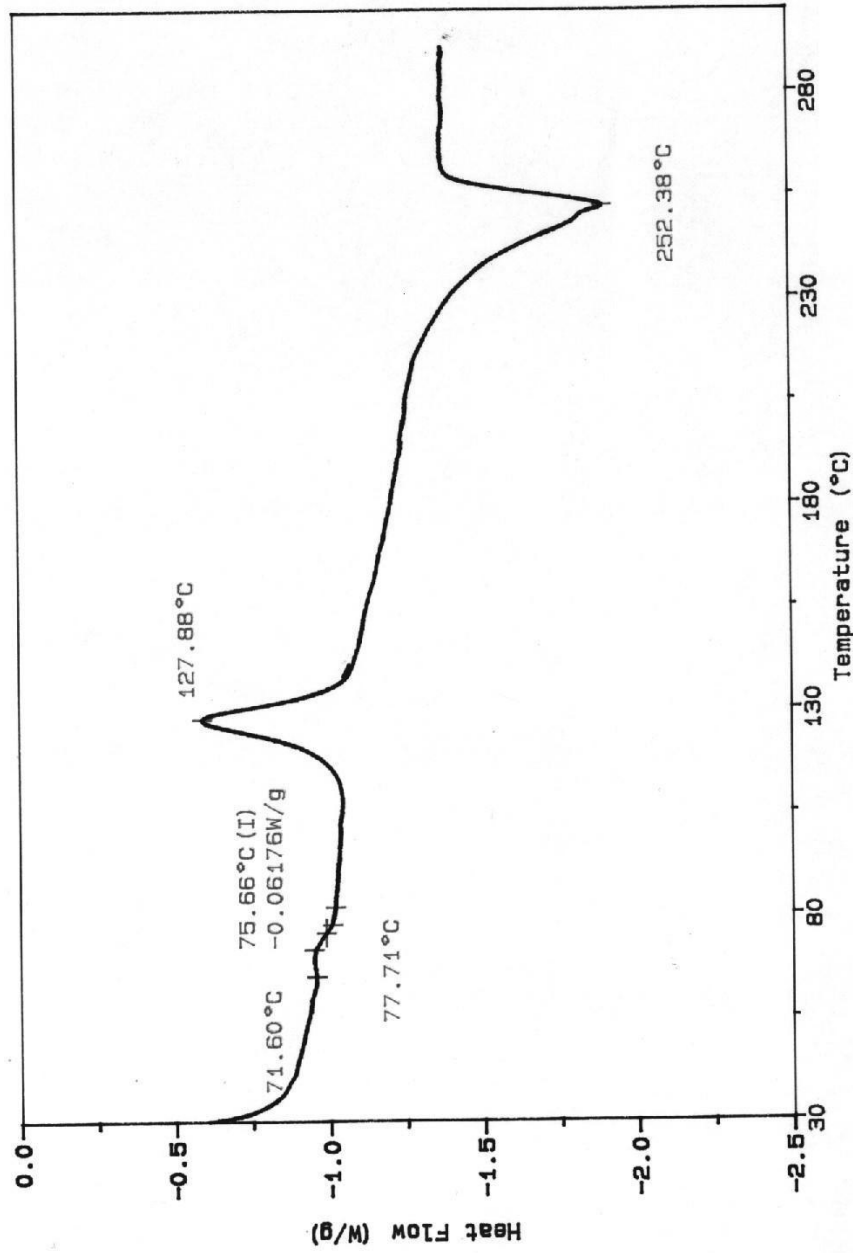


Figure 3.4 DSC Thermogram of Spun Fiber from BGPET

The thermogram of the fiber made from BGPET shows (Figure 3.4) a crystallization peak whereas BGPET did not. This is due to thermal history of the material where it is melted in the fiber formation process and solidified quickly before full crystallization during spinning.

The BGPET with LCP, the R-PET and the LCP added R-PET did not show any crystallization peak and all of them demonstrated sharp and strong melting endotherms. In Figure 3.5 the DSC thermogram of BGPET+1%LCP which is blended in the reactor and is let to cool slowly apparently achieved a maximum amount of crystallinity under the given conditions so no crystallization peak is observed. The sharpness of the melting peak indicates a good amount of crystallite formation. BGPET+2%LCP shows a similar behaviour in Figure 3.6 with a lower melting temperature and not as sharp a melting peak as in the previous sample. It is interesting to note that, however, small one should be able to notice the immiscible LCP phase melting endotherm around 210<sup>0</sup>C does not exist [27]. This observation can suggest that the most of the LCP is incorporated into the PET polymer chain through various esterification reactions and does not exist as a separate phase. A similar lack of a separate LCP melting peak is observed in the following figures.

In Figure 3.7, 3.8 and Figure 3.9 R-PET, R-PET+1%LCP and R-PET+2%LCP respectively have no crystallization peak and all have sharp melting peaks. It is not possible to comment the thermal history of the recycled sample but, LCP added R-PET is blended similar to other blends with a slow rate of cooling in the reactor that allows a maximum possible amount of pre-crystallization. The area of the melting peak suggests that as LCP is added amount of crystallinity decreases although no accurate analysis is carried out in this study.

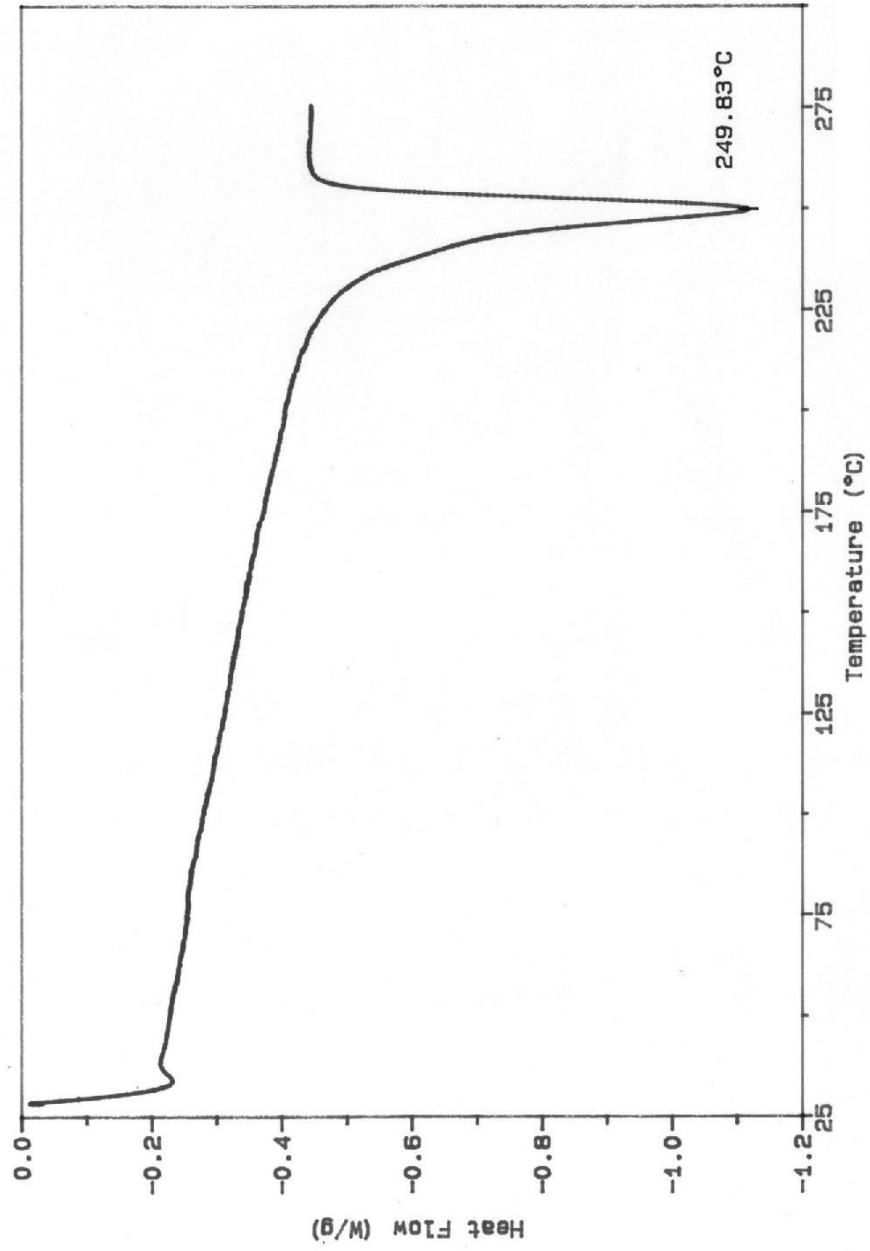


Figure 3.5 DSC Thermogram of BGPET +1% LCP Blend Fiber

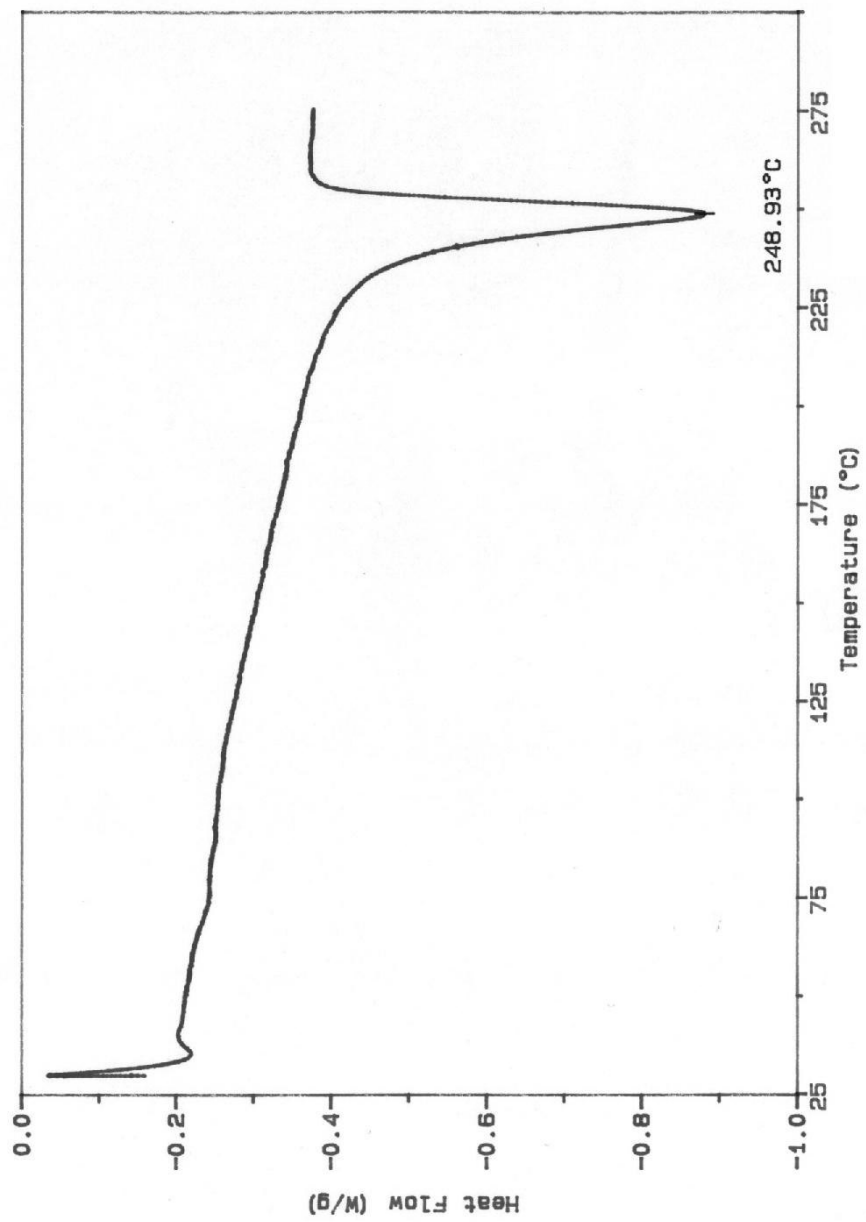


Figure 3.6 DSC Thermogram of BGPET + 2% LCP Blend Fiber

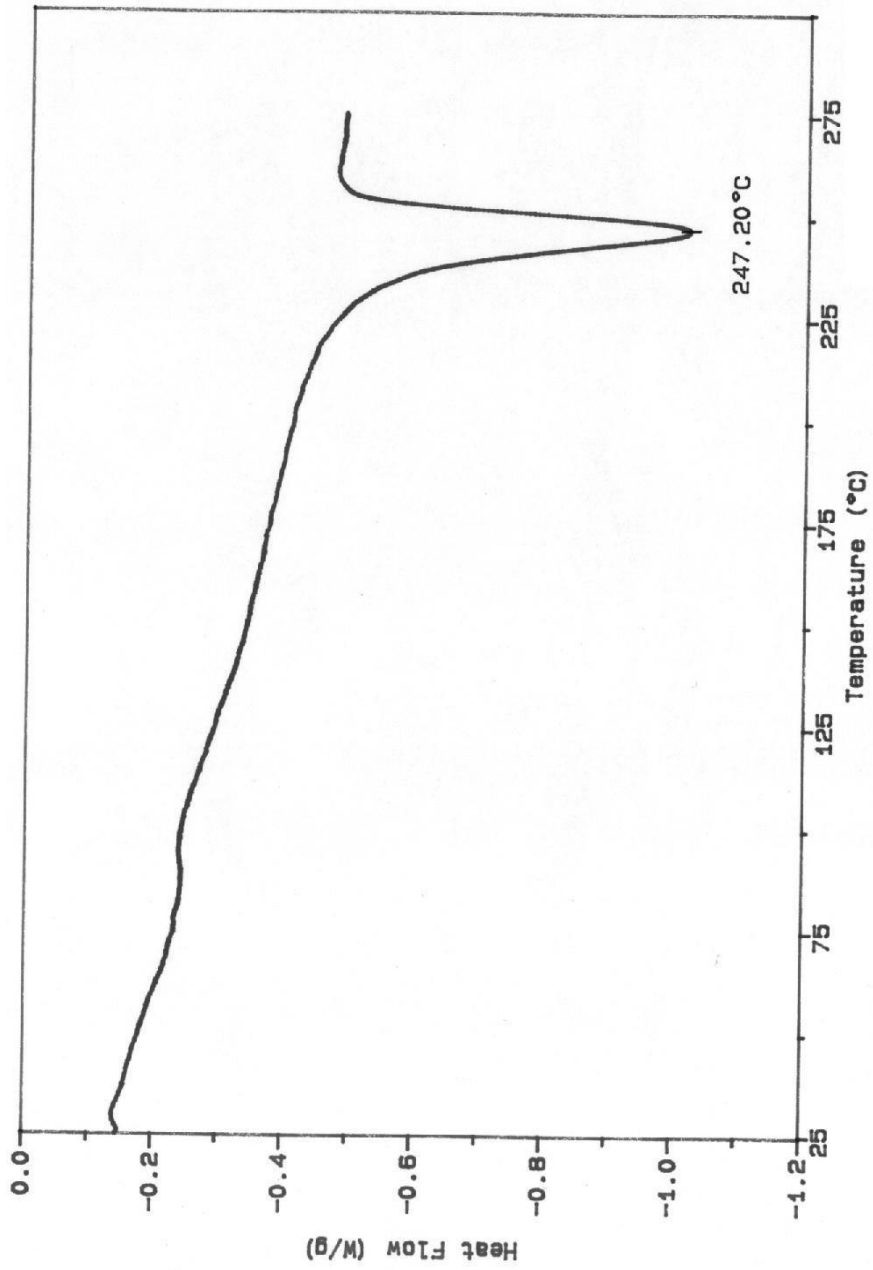


Figure 3.7 DSC Thermogram of Recycled PET (R-PET)

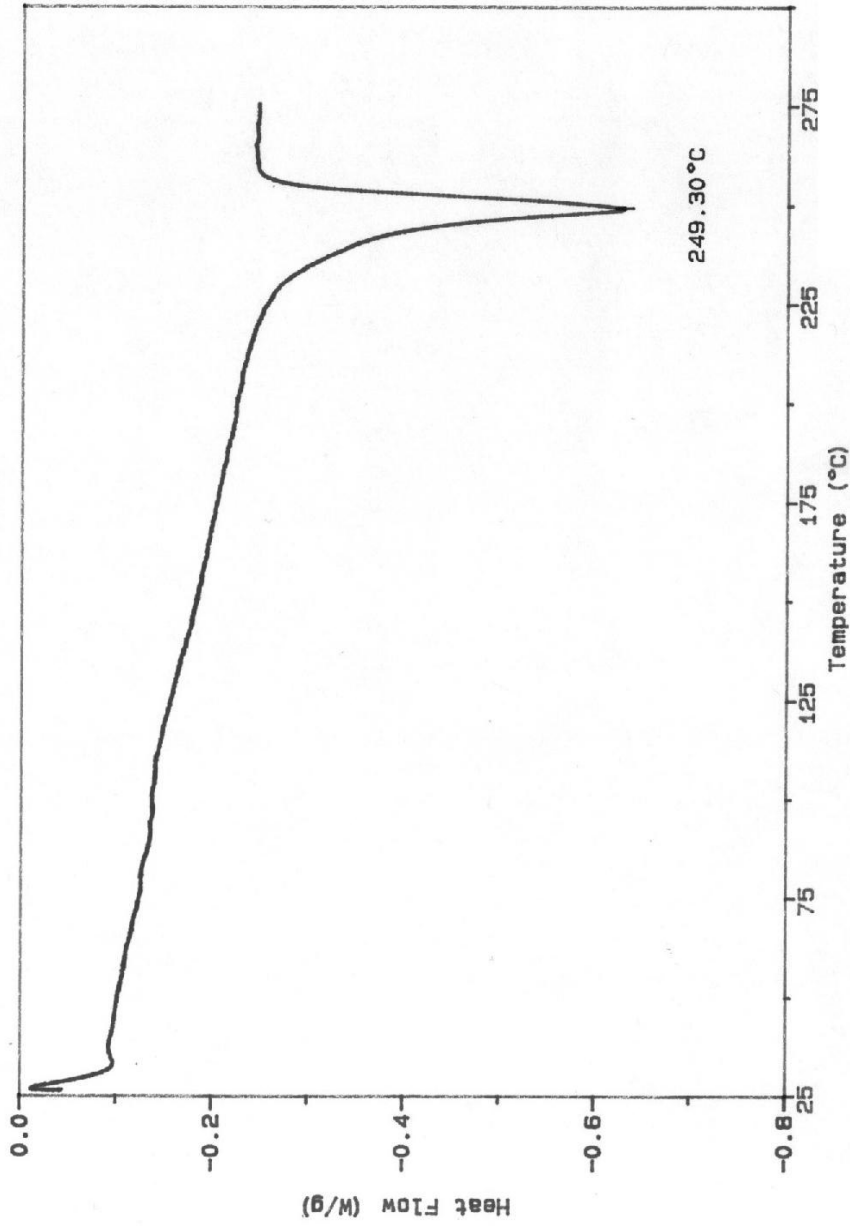


Figure 3.8 DSC Thermogram of R- PET + 1% LCP Blend Fiber

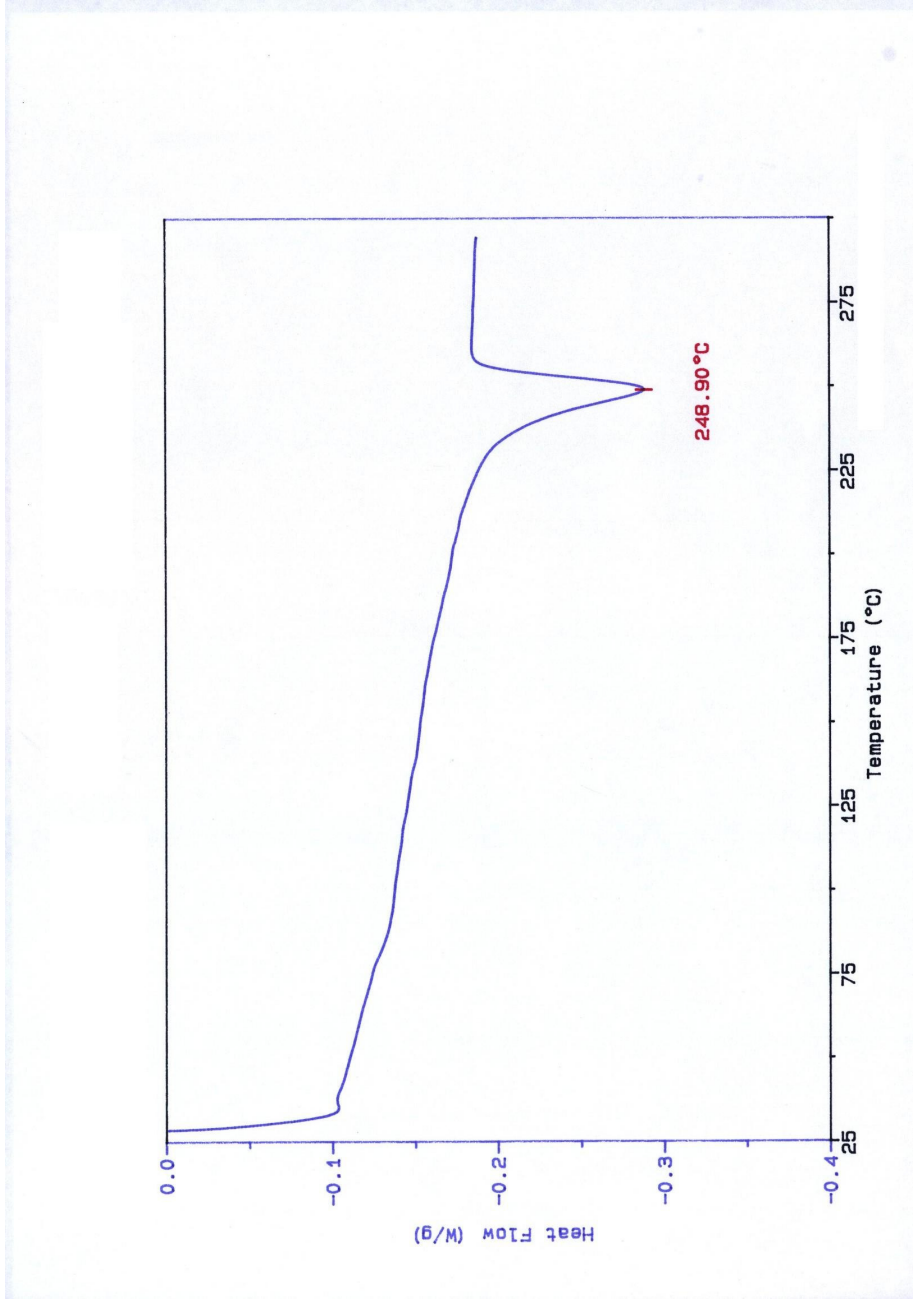


Figure 3.9 DSC Thermogram of R-PET + 2% LCP Blend Fiber

### 3.4 SEM Results

The fibers in this study are spun at a low speed compared to commercial spinning processes, therefore, the crystallinity and chain orientation that can be achieved is low. Chain extension during spinning occurs at the spin line where an elongational flow regime exists which is much longer and an order of magnitude faster than that is achieved under laboratory conditions. The fibers obtained in this study can, nevertheless, be compared with each other in terms of fiber morphology and mechanical properties.

The fibrillation at the ruptured surface of the fiber grade PET can be seen in Figure 3.10. The skin which cools fast is smooth and amorphous. Compared to fiber grade PET fiber (Fig.3.11) the bottle grade fiber in Figure 3.12 has a ductile rupture. One can see the axial lamellar structures in both fibers.

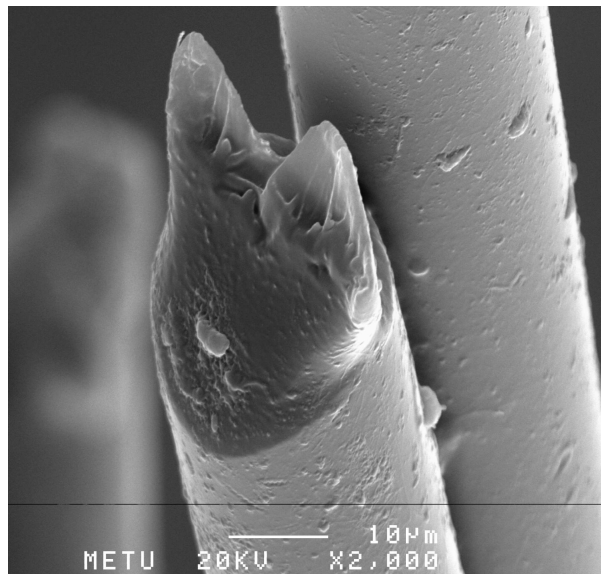


Figure 3.10 SEM Microphotograph of the fiber from FGPET

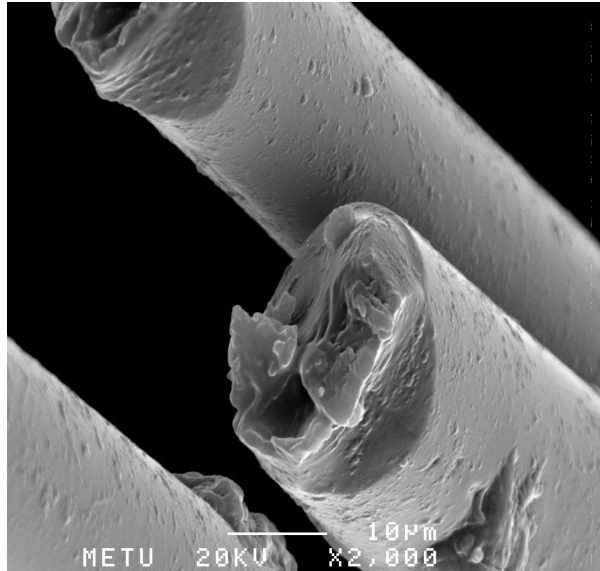


Figure 3.11 SEM Microphotograph of FG PET fiber with lamellar structure.

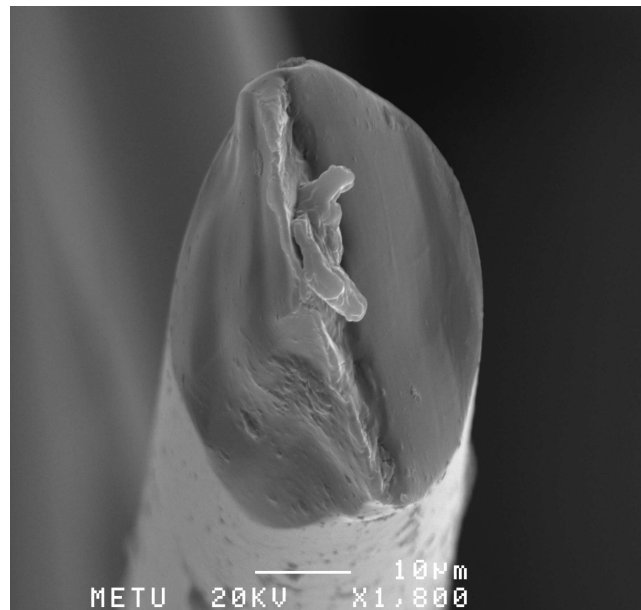


Figure 3.12 SEM Microphotograph of the fiber from BG PET

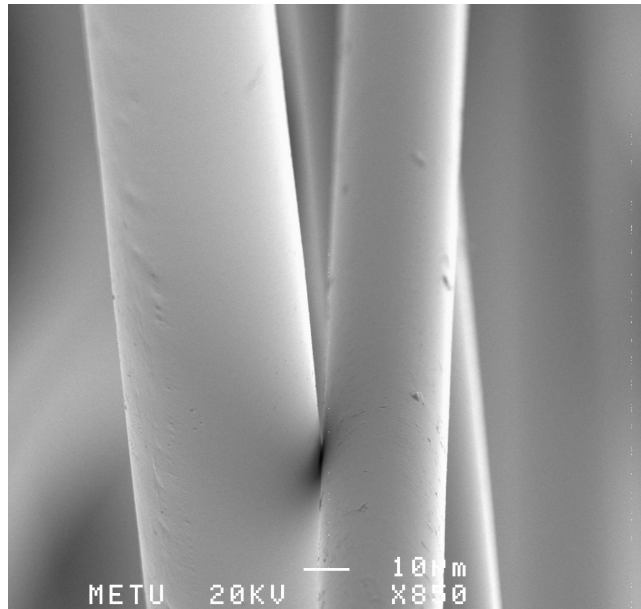


Figure 3.13 SEM Microphotograph of the fiber from BGPET with smooth skin

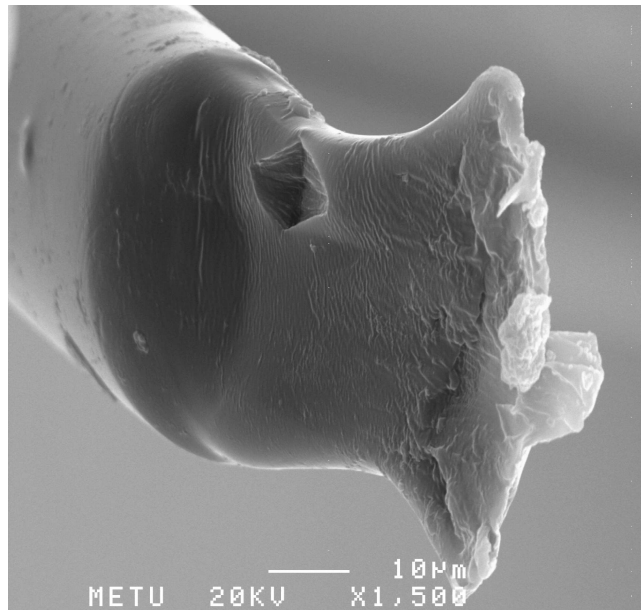


Figure 3.14 SEM Microphotograph of the fiber from BGPET with ductile rupture

The BGPET shows no fibrillation and lamellar structure at its ruptured surface; its skin is very smooth and bland with no specific character (Fig. 3.12, 3.13 and 3.14). The LCP containing blends in Figures 3.15, 3.16 have both ductile rupture and apart from the other fibrillation at the rupture points.

The character of the recycled PET fibers in Figure 3.17 and 3.18 show almost no lamellar structures. A collection of recycled PET fibers are given in Figure 3.19.

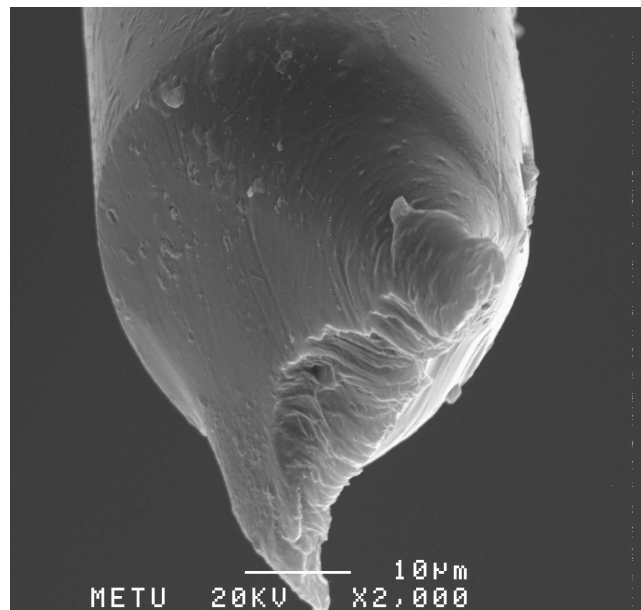


Figure 3.15 SEM Microphotograph of the fiber from BGPET+ 1%LCP with lamellar structure

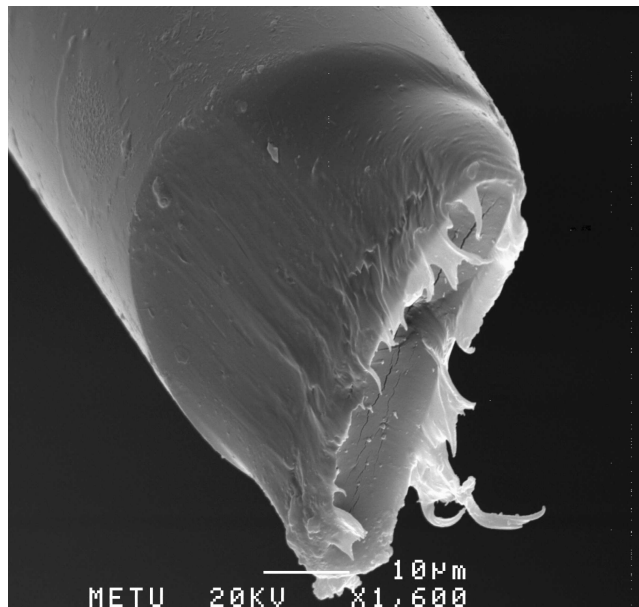


Figure 3.16 SEM Microphotograph of the fiber from BGPET+1%LCP blend fiber that shows fibrillation

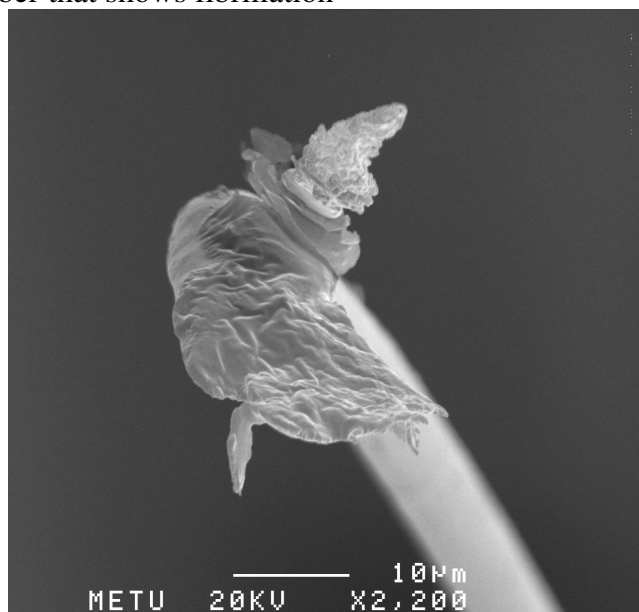


Figure 3.17 SEM Microphotograph of a thin R-PET fiber

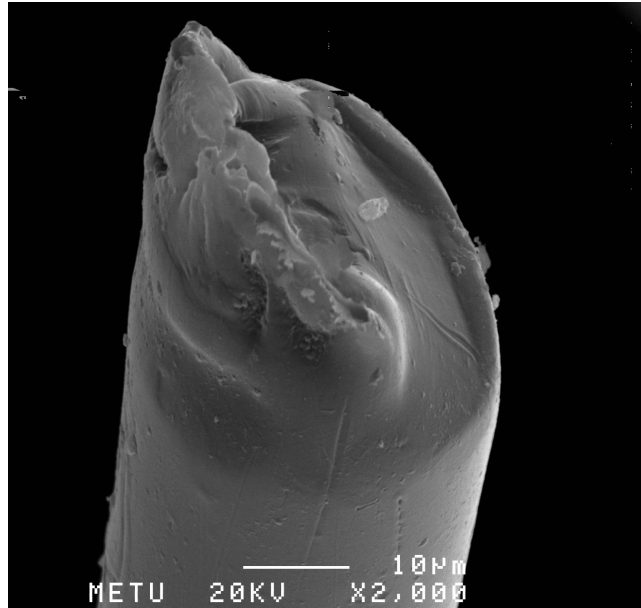


Figure 3.18 SEM Microphotograph of R-PET fiber with no lamellar structure

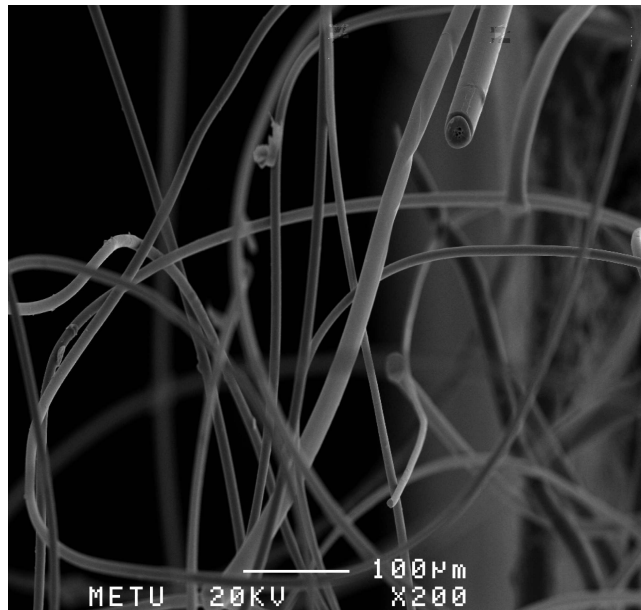


Figure 3.19 SEM Microphotograph of a collection of R-PET fibers

### 3.5 Tensile Properties of the Fibers

The tensile strengths of spun and drawn fibers are given in Table 3.4. Recycled PET (R-PET) and 1%LCP added R-PET are compared FG PET fibers. Addition of small amount of LCP increases the tensile properties of recycled PET significantly.

Table 3.4 Maximum Tensile Strength and % Strain at Break Values of the Fibers

	MAX.TENSILE STRENGTH (MPa)	% STRAIN at BREAK
FG PET	43.0	1.75
R-PET	33.7	2.78
R- PET +1% LCP Blend	38.8	1.90

As shown in Figure 3.20 the maximum tensile strength, percent strain at break and the modulus values of the LCP added R-PET is in between the FG PET and R-PET. The LCP addition, therefore, has achieved the desired effect in improving the fiber forming properties of the recycled polymer. The actual performance should of course be tested in an industrial scale production facility.

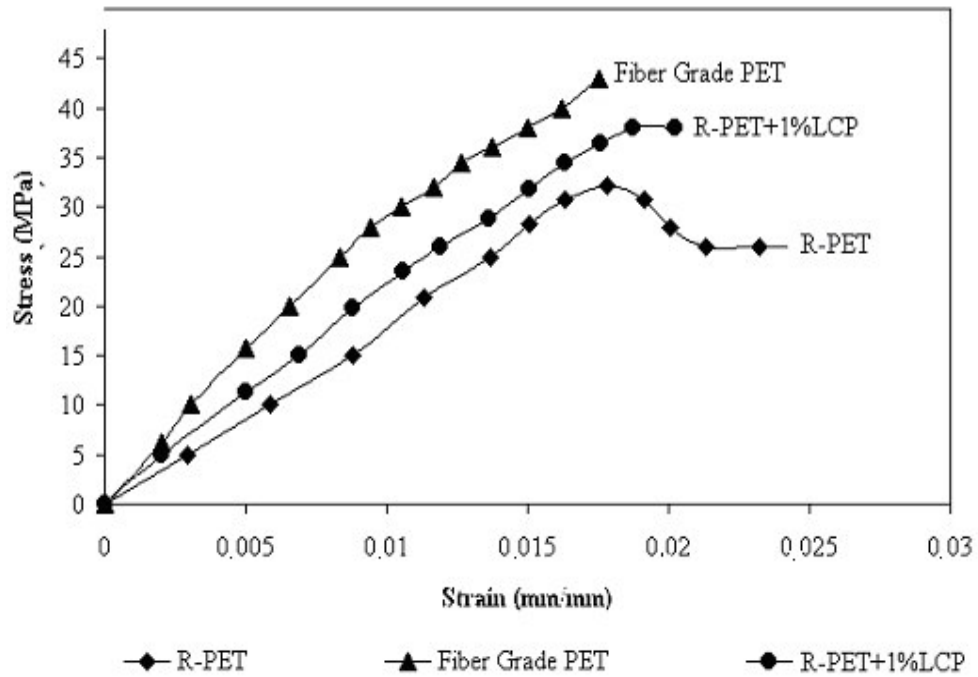


Figure 3.20 Stress-strain curves for R-PET, FGPEt and R-PET+1%LCP blend fibers

The bar graphs of the mechanical properties of the as-drawn fibers tested are given in Figures 3.21, 3.22 and 3.23. In summary the LCP addition has increased the modulus and the maximum stress values and decreased the maximum strain of the samples.

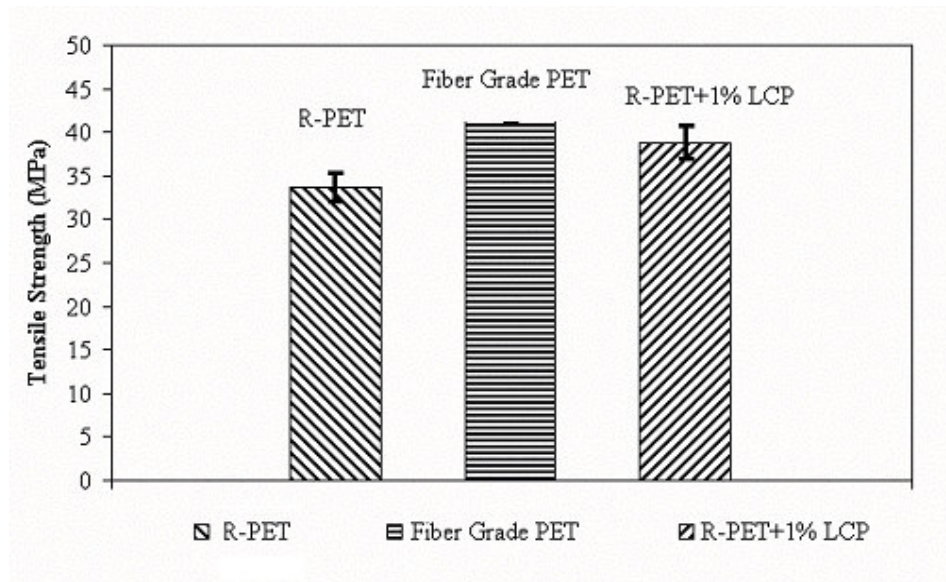


Figure 3.21 Variation of tensile strengths for R-PET, FG PET and R-PET +1%LCP blend fibers

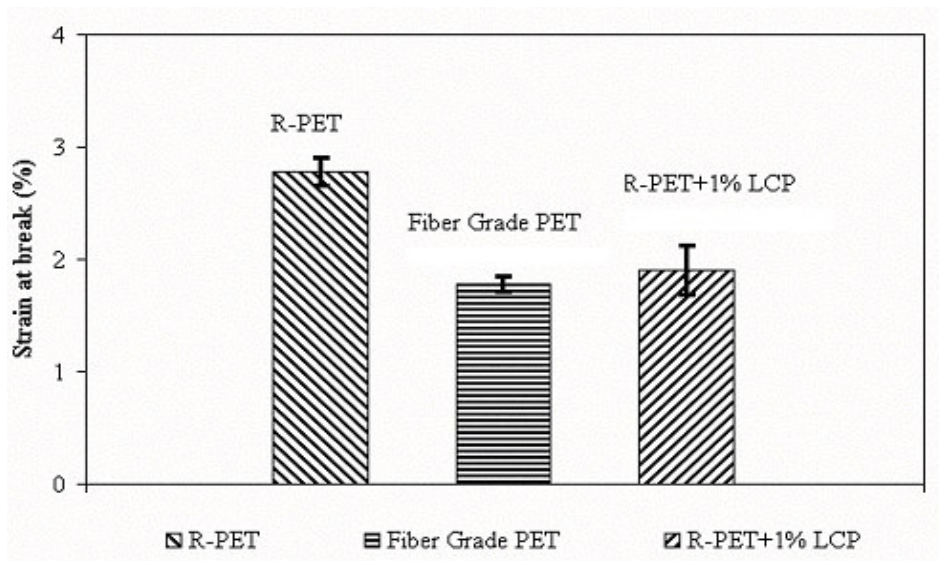


Figure 3.22 Variations of strain at break values for R-PET, FGPET and R-PET+1%LCP blend fibers

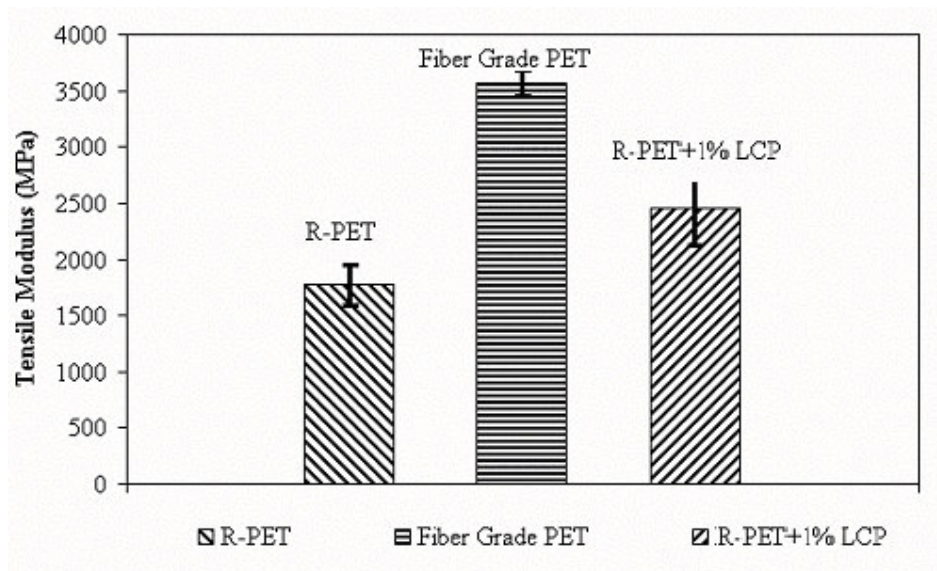


Figure 3.23 Variation of tensile modulus for R-PET, FG PET and R-PET +1%LCP blend fibers

### 3.6 Wide Angle X- Ray Test Results

It was not possible to obtain satisfactory WAXD data due to the difficulty in sample preparation in sufficiently powder form. The peak at around  $2\theta = 37^\circ$  belongs to the aluminum sample powder container (Figure 3.24). Around  $20^\circ$  the very wide bulge can be interpreted as a pseudo-hexagonal order that is quite weak. This issue will be tackled in more detail in the forthcoming studies. All the other samples gave similar results to that observed in Figure 3.24.

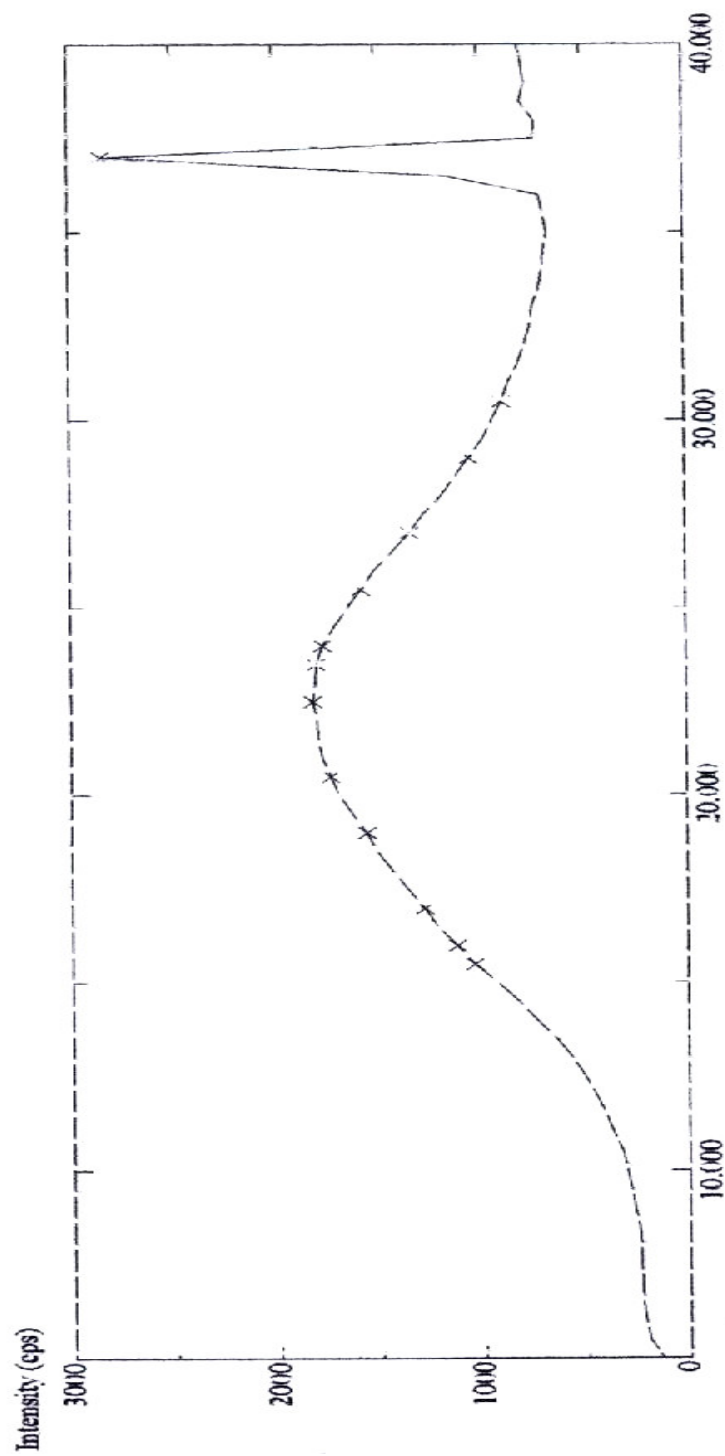


Figure 3.24 WAXD spectrum of R-PET + 1% LCP; intensity vs.  $2\theta$

## CHAPTER 4

### CONCLUSIONS

In this study we initiated a study to improve the properties of recycled PET to be used as continuous or discontinuous fiber stock. We have tackled many aspects of the problem and obtained encouraging preliminary results and prepared the required experimental set-ups and the methods.

The basic conclusions drawn from this work are as follows;

1. The X7G (LCP) addition in very small amounts has improved the fiber forming properties of regenerated PET as determined by mainly tensile tests and fibrillation observed in SEM studies. Also the DSC results indicated an increased amount of crystallinity.
2. Throughout this study we have used the term 'blend' to describe the LCP added samples as a matter of convenience. The DSC results however suggest that the LCP phase may not exist separately as a distinct phase, but, be incorporated molecularly into the PET polymer chain. This factor needs to be studied by other techniques such as Size Exclusion Chromatography, FTIR and Proton and Carbon NMR.
3. According to WUSS Effect (Wind-up Speed Suppression) the presence of a small amount of second phase in polymer melts suppresses

crystallization in the spin-line and makes possible to operate the spinning machines at much higher speeds that increases productivity. An important observation in this study is that a prolonged blending operation at a relatively high temperature (30 minutes and 275<sup>0</sup>C in our study) changes WUSS since the LCP component is no longer a very distinct phase, probably, most of it is incorporated to the very predominant matrix PET phase. This finding has to be taken into account for the design of new fiber forming technology.

4. Our initial tests indicate that it is at least possible to obtain discontinuous yarn from LCP added regenerated PET.

## REFERENCES

- [1] Qin Y., (1995), *Polymer for Advanced Tech.*, 7, 151-159.
- [2] Nakai A., Shiwaku T., Wang W., Hasegawa H., Hashimoto T., (1996), *Polymer*, 37, 2259-2272.
- [3] Li J.X., Silverstein M.S., Hiltner A., Baer E.,(1992), *J. Appl. Polym. Sci.*, 44, 1531-1542.
- [4] Mehta S., Deopura B.L., (1993), *J. Appl. Polym. Sci.*, 47, 857-866.
- [5] Xiao C., Zhang Y., Takahashi T., (2002), *J. Appl. Polym. Sci.*, 83, 394-400.
- [6] Borun L., Pan L., He X., (1997) , *J. Appl. Polym. Sci.*, 66, 217-224.
- [7] Fann Daw-Ming, Huang S.K., Lee Jiunn-Yih, (1996), *J. App. Polym. Sci.*, 61, 1375-1385.
- [8] Subramanian P.M., (2000), *Resources, Conservation and Recycling*, 28, 253-263.
- [9] Oramiehie A., Mamizadeh A., (2004), *Polymer International*, 53, 728-732.

- [10] Lusinchi J.M., Pietrasanta Y., Robin J.J., Boutevin B., (1998), J. Appl. Polym. Sci., 69, 657-665.
- [11] Zoran S.P., Farris R., (1995) , J. Appl. Polym. Sci., 58, 1077-1085.
- [12] De Gennes P., Prost J., (1993), The Physics of Liquid Crystals Clarendon, New York.
- [13] Ericksen J.L., (1960), Arch.Ration.Mech.Anal., 4, 231.
- [14] Leslie F.M., Quart, (1996), J of Mech.Appl.Math., 19, 357.
- [15] Nobbs J.H., Bower D.I., Ward I., (1976), Polymer, 17, 25.
- [16] Henneke M., Fuhrmann, Kurz K., (1989), Polymer, 30, 1072.
- [17] Le Bourvellee G., Monnerie L., Jarry J.P., (1986), Polymer, 27,1712.
- [18] Cheng S.Z.D., Li F., Li Y.C., McCreight W.K., Yoon Y.and Harris W.F., Fibers from Liquid Crystalline Polymers, Cambridge Univ.Press, USA.
- [19] Brody H., (1986), J. Appl. Polym. Sci., 31 ,2753-2768.
- [20] Brody H., Proceedings of the International Fiber Science and Tech., Aug.20-24, 1985, Hakone, Japan, 230.
- [21] Perez G., Jung E., Proceedings of the International Fiber Science and Technology, Aug.20-24, 1985, Hakone, Japan, 64.
- [22] Şengönül M., (1998), Master Thesis, METU.

- [23] Strong A.B., 'Plastics :Materials and Processing', Prentice Hall, New Jersey, (2000).
- [24] Develioğlu T., (1998), Master Thesis, METU.
- [25] Morton W.E., Hearle J.W.S., (1975), Physical Properties of Textile Fibers, England.
- [26] Keyfoğlu A.E., (2004), Master Thesis, METU.
- [27] Ateş C., (2002), Master Thesis, METU.
- [28] Sajkiewicz P., (1990), Fiber World, 3, 235-247.
- [29] Mirowska M., (1991), Fiber World, 12, 112-126.
- [30] Mehta S., Deopura B.L., (1995), J. Appl. Polym. Sci., 56, 169-175.
- [31] Sasse F., Emig G., (1998), Chem. Eng. Tech., 10 ,777-789.
- [32] Miles S., (1987), J. Appl. Polym. Sci., 34, 2793-2807.
- [33] Fann Daw-Ming, Huang S.K., Lee Juinn-Yih, (1996), J. Appl. Polym. Sci., 61, 261-271.
- [34] Zoran S.P., Farris R., (1995), J. Appl. Polym. Sci., 58, 1349-1363.
- [35] Min K., White J.L., Fellers J.F., (1986), J. Appl. Polym. Sci., 29,501.

- [36] Hibi S., Maeda M., Kubota H., Miura T. *Polymer*, (1977), 18,137.
- [37] Hongu T., Phillips G.O., *New fibers*, (1990), Ellis Horwood, New York.
- [38] Muramatsu H., & Krigbaum W.R., (1987), *J. Poly. Sci. Part B: Polym. Phy.*, 25, 803.
- [39] Viola G.G., Baird D.G. & Wilkes G.L., (1985), *Polym. Eng. Sci.*, 25, 888.
- [40] Cuculo J.A. & Chen G.Y. (1988), *J. Polym. Sci. Part B: Polym. Phy.*, 26, 179.
- [41] Dibenedetto A.T. & Stachowski M.J., (1997), *Polym. Eng. Sci.*, 37, 252.
- [42] Seigmann A., Dagan A. & Kenig S., (1985), *Polymer*, 26, 1325.
- [43] Viney C. & Windle A.H., (1982), *J. Mater. Sci.*, 17, 2661-2670.
- [44] Gohil R.M., Salem D.R., (1993), *J. Appl. Polym. Sci.*, 47,1989.
- [45] Henneeke M.,Fuhrmann , (1982 ), *Polymer*, 23, 797.
- [46] Sonnenschein M.F., Roland C.M., (1990), *Polymer*, 31, 2023.
- [47] Yerlikaya Z., (1998), *Phd. Thesis*, Gazi Uni.

## APPENDIX

### Tensile Strength Values

#### R-PET

Sample	Diameter (mm)	Tensile Strength (MPa)	Yield Strain (%)	Strain at break (%)	Tensile Modulus (MPa)
1	8.60E-02	32.5	1.30	2.80	2500
2	8.60E-02	32.4	1.40	2.90	1500
3	8.60E-02	36.5	1.30	2.80	1589
4	8.60E-02	32.8	1.21	2.80	1750
5	8.60E-02	32.5	1.33	2.70	1482
6	8.60E-02	35.6	1.40	2.80	1986
7	8.60E-02	32.3	1.41	2.70	1685
8	8.60E-02	32.3	1.45	2.90	1789
9	8.60E-02	34.8	1.28	2.70	1990
10	8.60E-02	35.4	1.36	2.70	1450

Average:	33.70	1.34	2.78	1772.0
SDEV	1.67	0.07	0.08	320.90
Max	35.37	1.42	2.86	2093.0
Min	32.04	1.27	2.70	1451.2

#### FGPET

Sample	Diameter (mm)	Tensile Strength (MPa)	Strain at break (%)	Tensile Modulus (MPa)
1	0.076	44.8	1.77	2531
2	0.076	40.8	1.85	2205
3	0.076	41.2	1.73	2382
4	0.076	44.2	1.75	2526
5	0.076	40.2	1.65	2438
6	0.076	41.1	1.68	2446
7	0.076	44.2	1.69	2615
8	0.076	43.8	1.80	2433
9	0.076	45.6	1.85	2465
10	0.076	44.5	1.75	2543

Average:	43.04	1.75	3562.5
SDEV	1.98	0.07	319.80
Max	45.02	1.82	3882.3
Min	41.07	1.68	3242.7

**R-PET+1  
%LCP  
BLEND**

Sample	Diameter (mm)	Tensile Strength (MPa)	Strain at break (%)	Tensile Modulus (MPa)
1	0.12	38.2	1.99	3254
2	0.12	39.3	1.85	3895
3	0.12	36.0	2.30	3500
4	0.12	40.0	1.75	3600
5	0.12	40.2	1.66	3369
6	0.12	41.1	1.68	3452
7	0.12	35.5	2.20	3020
8	0.12	41.2	2.00	3555
9	0.12	38.2	1.85	3986
10	0.12	38.6	1.75	3994

Average:	38.83	1.90	2458.5
SDEV	1.95	0.22	111.90
Max	40.78	2.12	2570.4
Min	36.88	1.69	2346.5